Investigating the effects of nitric oxide upon antibiotic susceptibility in pathogenic *Escherichia coli*

Thesis for MSc by Research in Microbiology

School of Biosciences

University of Kent

Ayrianna Woody

2019

Word Count: 19,666

Declaration

I confirm that no part of this thesis has been submitted in support of an application for any degree or other qualification of the University of Kent, or any other University or Institution of learning.

Ayrianna Woody

16th August 2019

Abstract

A 30-year void in antibiotic discovery coupled with rampant antimicrobial resistance (AMR) among multi-drug resistant pathogens has created what is known as the Antimicrobial Resistance Crisis. Recent evidence strongly suggests aerobic respiration is required for bactericidal antibiotics to effectively kill bacteria via promoting generation of excess reactive oxygen species. Given that the immune system releases the potent respiratory inhibitor nitric oxide (NO) to combat pathogens, it is crucial to study how clinically relevant bacteria respond to an environment where a respiratory inhibitor (NO) is present along with an antibiotic.

Herein, four hypotheses were tested to investigate how antibiotic susceptibility in respiratory mutant *Escherichia coli* strains were influenced by NO. To investigate the antagonistic effects of a bactericidal aminoglycoside and NO, viability assays and oxygen consumption measurements were undertaken in the presence and absence of GSNO, a NO-donor, and gentamicin. Results clearly show *E. coli* exhibited protection from the lethal effects of gentamicin when oxidative phosphorylation was halted. Furthermore, the NO-tolerant respiratory oxidase cytochrome *bd*-I (encoded by *cydAB*) was shown to sensitize *E. coli* to antibiotics in the presence of GSNO. To investigate if GSNO offered relief from excess reactive oxygen species stemming from gentamicin-mediated hyperactivation of respiration, reactive oxygen species were carefully measured after treatment with gentamicin in the presence and absence of GSNO. Interestingly, GSNO stimulated excess reactive oxygen species rather than diminished; therefore, an alternative hypothesis is offered: aminoglycosides utilize the generation of the proton motive force to enter the cell to perform the primary mode of action to kill bacteria. NO-mediated respiratory inhibition may diminish the proton motive force thus gentamicin is unable to efficiently enter the cell and kill. This work supports the link between aerobic respiration and bactericidal antibiotic function through a reactive oxygen species-independent pathway and demonstrates the role the immune system may have in antibiotic efficacy.

Acknowledgements

To begin, I would like to thank Dr. Mark Shepherd for his seemingly endless support and guidance throughout this year. Thank you for the opportunity to study and contribute to the work conducted in your lab and encouraging me to work and develop my skills as a researcher. I would also like to thank the Shepherd and Robinson labs for all the help with procedures, method development, and difficult questions that allowed me to expand my knowledge to find creative solutions to persistent problems. Thank you for the great memories from the Christmas party to finally becoming microbiologists that have made a (tasty) brew. I would especially like to thank Calum Webster for allowing me to talk his ear off in the lab every day and share his experience with me where I was lacking.

I would like to thank the people with whom I have formed lifelong bonds with. Thank you for supporting me in this degree, allowing me to vent and fuss when I needed to, and showing me how amazing a strong group of friends can be in times of stress and doubt. Thank you for being my home away from home.

Lastly, but by no means least, I would like to thank my family. The support they have given me did not begin when I decided I wanted to move across the ocean to a country I have never been before to study for a year- they have always been there for me and the decisions I have made in my life. My father has never doubted my abilities and my determination to achieve and my mother is forever my rock always knowing what to say in my times of need. Thank you for always putting your children first and allowing me to thrive and become the person I am today.

Presentations

Poster Presentation:

Woody, Ayrianna; Shepherd, Mark. The Immune System Helps Bacteria Escape Antibiotics: It Should NO Better. *University of Kent Researchers' Showcase, Canterbury, England, 2019.*

Abbreviations

ADP	Adenosine Diphosphate
AMR	Antimicrobial Resistance
Ap	Ampicillin
ATP	Adenosine Triphosphate
Cm	Chloramphenicol
Cm^R	Chloramphenicol Resistance
ESBL	Extended-spectrum β-Lactamase
ETC	Electron Transport Chain
Gm	Gentamicin
GSNO	*S*-Nitrosoglutathione
HGT	Horizontal Gene Transfer
KO	Knockout
MDR	Multi-drug Resistant
MGE	Mobile Gene Elements
NO	Nitric Oxide
PMF	Proton Motive Force
ROS	Reactive Oxygen Species
TCA	Tricarboxylic Cycle
Tet	Tetracycline
UPEC	Uropathogenic *Escherichia coli*
UTI	Urinary Tract Infections

Table of Contents

List of Figures

List of Tables

List of Equations

Chapter 1

Introduction

1.1. The Antimicrobial Resistance Crisis

1.1.1. Antibiotic resistance overview

Penicillin was first identified as an antibiotic by Alexander Fleming in 1928 when he observed a *Penicillium* fungus excrete an antimicrobial substance on an agar plate (Fleming, 1950). After roughly a decade of international collaboration, penicillin was effectively mass produced and revolutionized the medical world in time to aid in World War II (Gaynes, 2017). Though the introduction of penicillin ushered in a "golden" era of antibiotic discovery, it was shortly followed by widespread resistance and introduced the now well-known arms race to keep up with resistance mechanisms employed by microbes deemed the antimicrobial resistance (AMR) crisis (Nathan & Cars, 2014) (van Hengel & Marin, 2019) (Martens & Demain, 2017).

With the use of various antibiotics spanning the years since penicillin was deployed for clinical use, there is a threat of proceeding to a post-antibiotic era due to rampant resistance by microbes (Figure 1.1). Identified problems contributing to AMR include increasing travel of humans, overuse and over-prescription of antimicrobials, and lack of education for the public (Rather, et al.,

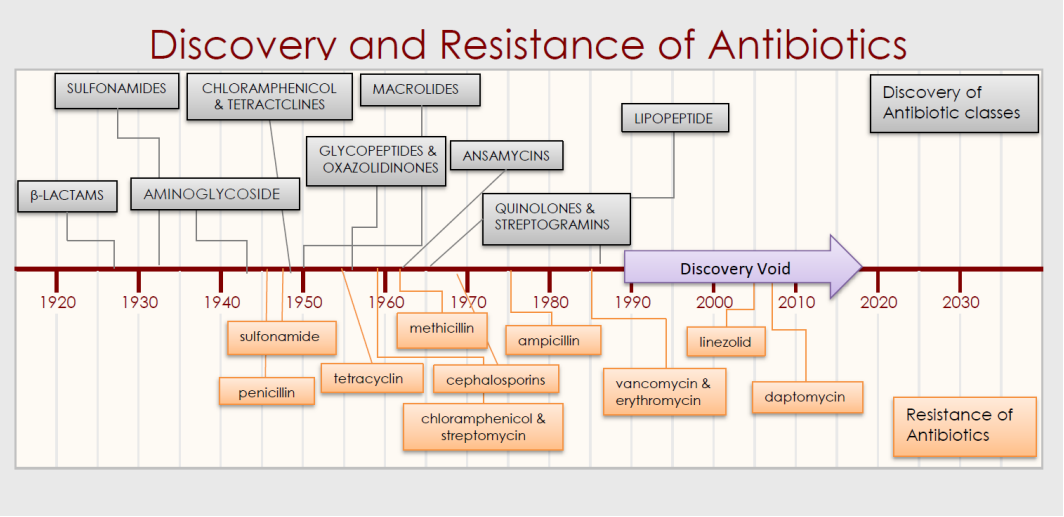

Figure 1.1 Timeline of the discovery and bacterial resistance to common classes of antimicrobials*. With a discovery void in antibiotics spanning close to 30 years, the threat of a post-antibiotic era is imminent. Adapted from Public Health England (2015).*

2017) (Michael, et al., 2014). Microbial life is evolving resistance to antimicrobials faster than new therapeutics are being produced. Indeed, less than five new antibiotics have been fully developed into a product since 2009, and fewer still have the ability to treat a broad-spectrum of bacterial infections without dangerous side effects (Boucher, et al., 2013) (Fair & Tor, 2014) (Fernandes & Martens, 2017). To tackle this crisis, researchers must understand the mechanisms that bacteria use to evade current antibiotics and exploit this knowledge to create new therapeutics.

1.1.2. Mechanisms of antibiotic resistance

With the introduction of more antibiotics, multi-drug resistant (MDR) organisms have evolved and are recognized by numerous national and international health organizations as an imminent danger to society and the global economy (World Health Organization, 2014) (Public Health England, 2015) (Centers for Disease Control and Prevention, 2018). According to the antibiotic threats report from the Center for Disease Control and Prevention, there was an estimated 26,000 clinical cases involving extended-spectrum β-lactamase (ESBL)-producing Enterobacteriaceae with 1,700 (6.5%) of those cases ending in a fatality in the United States alone (2013). Additionally, 10 million lives are projected to be lost globally by 2050 due to resistant microbes resulting in £66 trillion in lost global productivity (O'Neill, 2015).

1.1.2.1. The ST131 clonal type of *E. coli*

The study herein is focused on the ST131 sequence type of *Escherichia coli*, a globally disseminated clonal type that is known to spread rapidly and frequently exhibit resistance to fluoroquinolones, aminoglycosides, and trimethoprim-sulfamethoxazole combinations (Petty, et al., 2014). *E. coli* ST131 is also associated with a highly virulent producing CTX-M-15 type ESBL, one of the most invasive resistant enzymes globally (Forde, et al., 2014). The most comprehensive characterization from the ST131 sub-clonal group has been conducted on the serotype O25b:H4 uropathogenic (UPEC) strain EC958, which was isolated from

Northwest England in 2005 from a urine sample of a young girl (Totsika, et al., 2011). This strain contains a diverse repertoire of virulence associated genes including adhesins, autotransporter proteins, and type I fimbriae (used to invade and attach to bladder cells) (Forde, et al., 2014). Due to the high virulence and MDR associated genes located on the large plasmid (~134 kb) harbored by this strain, it has been a major contributor to urinary tract and blood infections in Europe, Asia, Africa, North America, and Australia (Totsika, et al., 2011) (Rogers, et al., 2011). The clinical relevance of this strain is extremely important when discussing mechanisms of resistance and how to move forward in developing new therapeutics to combat MDR pathogens.

Resistance to naturally occurring antimicrobial compounds is to be expected from pathogens co-existing with other microbial life. AMR does not highlight naturally occurring resistance, rather it focuses on acquired resistance in clinically relevant strains. Evolutionarily, bacteria have two main approaches to cope with the pressure from antimicrobials: genetic mutation and horizontal gene transfer.

1.1.2.2. Genetic mutations resulting in antimicrobial resistance

Antimicrobial resistance genes typically first occur in bacteria that produce antimicrobials thereby avoiding the toxic effects of the substance produced (e.g. Streptomyces). Over time, bacteria develop mutations or uptake genes from neighboring species that facilitate survival when exposed to an antimicrobial in their environment. Any mutations that occur can be costly to the cell; therefore, in general, minor mutational adaptations to the target of an antimicrobial prevail (Munita & Arias, 2016). Mutations occur randomly, thus the mutations that arise are diverse yet common resistance mechanisms seen in bacterial species include: changes in the antibacterial target, efflux pumps and porins, altered drug uptake, and changes in pathways the antibacterial might target (Table 1.1) (Munita & Arias, 2016) (Fernandez & Hancock, 2012). When a successful resistance mechanism arises, bacteria can "share" the mechanism through transfer and uptake of genes from external sources via horizontal gene transfer.

Table 1.1 *Modes of action and resistance mechanisms for common antibiotic classes*

Antibiotic Class	Mode of Action	Common Resistance Mechanism
β-Lactams	Substrate Analog in synthesis of Murein: Cell Wall Synthesis	Hydrolyze the β-lactam ring (Kong, et al., 2010)
Sulfonamides	Analog of PABA[3]: Folic Acid Synthesis	Amino acid substitution in *E. coli* (Skold, 2000)
Aminoglycosides	Binds to active site in rRNA: Protein Synthesis	Structural modification of antibiotic to inactivate (Kotra, et al., 2000)
Tetracyclines	Binds to A-site in 30S/50S ribosomes: Protein Synthesis	Efflux pumps and ribosomal protection from antibiotic (Speer, et al., 1992)
Chloramphenicol	Binds to peptidyl transferase in 50S ribosomal subunit: Protein Synthesis	Acetylation via CATs[4], efflux pumps, and phosphotransferase to inactivate drug (Schwarz, et al., 2004)
Macrolides	Binds to P-site in 50S ribosomal subunit: Protein Synthesis (Mazzei, et al., 1993)	Blocked ribosomal binding; efflux pump; drug inactivation (Leclercq, 2002)
Quinolones	Converting gyrase and topoisomerase IV into toxic enzymes: DNA degradation	Alteration of antibiotic; efflux pumps (Aldred, et al., 2014)

1.1.2.3. Horizontal gene transfer

Horizontal gene transfer (HGT) is the process via which bacteria, through several mechanisms, can share genes. Though mutation is how resistance initially occurs, HGT is the mechanism through which resistance spreads rapidly throughout a community and why antimicrobial resistance is so difficult to combat. The three main avenues bacteria can acquire foreign DNA are a)

[3] Para-Aminobenzoic acid
[4] Chloramphenicol acetyltransferase

transformation, b) transduction, and c) conjugation (Figure 1.2). Transformation occurs when free DNA is taken up by a bacterial cell; although very few clinically relevant strains can acquire foreign DNA this way (Munita & Arias, 2016). Transduction, the transfer of DNA through a bacteriophage, is another way antimicrobial resistance has been spread, although it is typically associated with the spread of virulence factors rather than resistance genes (Barlow, 2009).

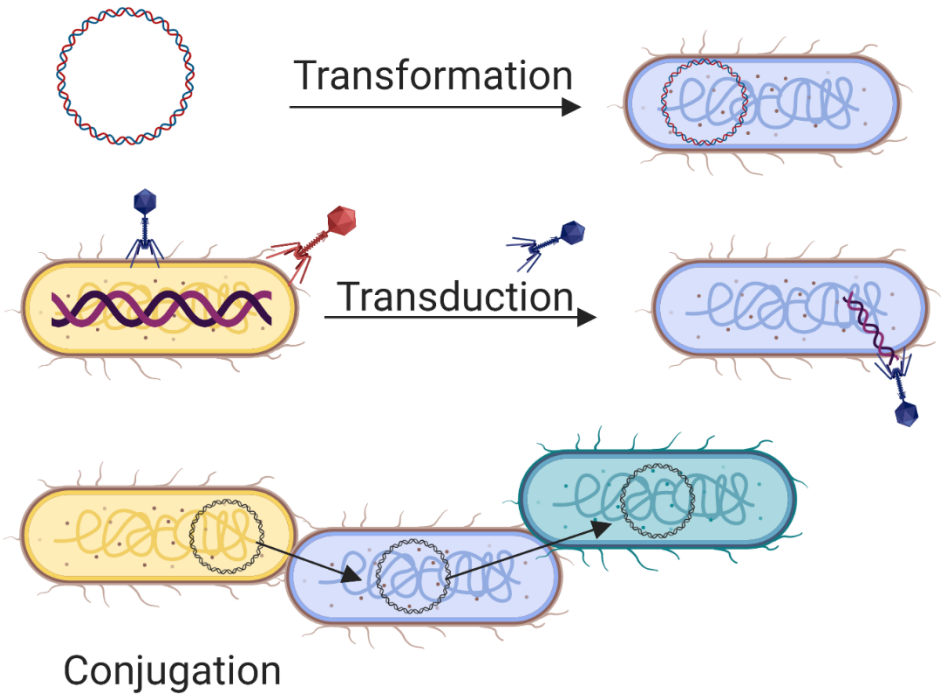

Figure 1.2 Horizontal gene transfer (HGT) occurs via three separate mechanisms. *When a bacterial cell acquires foreign DNA from the environment (transformation), when a bacterial cell receives foreign DNA from a bacteriophage (transduction), and when bacterial cells are in physical contact and transfer genes on a plasmid (conjugation).*

Though transformation and transduction have contributed substantially to AMR, conjugation is often credited for the vast and rapid spread of antimicrobial genes (Barlow, 2009) (Munita & Arias, 2016). Conjugation occurs when bacteria physically connect and transfer mobile gene elements (MGE) including conjugative plasmids and transposons (Munita & Arias, 2016). Plasmids are known to encode genes that confer resistance to every antibiotic class discovered (Barlow, 2009),

which highlights the potential for rapid spread of resistance and the urgent need for additional research on AMR.

One such area of research that requires a better understanding is the link between aerobic respiration and susceptibility to antibiotics. Previous work has established a robust link between oxidative phosphorylation and the lethality of a variety of antibiotic classes, with reactive oxygen species and antibiotic uptake rates implicated in the mechanisms of toxicity (Lobritz, et al., 2015) (Dwyer, et al., 2014). Hence, the processes of aerobic respiration will be introduced below, and evidence for a link with antibiotic resistance will be presented.

1.2. Aerobic Respiration in *Escherichia coli* and Antibiotic Susceptibility

1.2.1. Overview of respiration

As a facultative anaerobic pathogen, *E. coli* has developed numerous pathways to survive in the varied environments it inhabits. *E. coli* can survive in fully aerated as well as completely anoxic conditions and possesses a sophisticated system to monitor, adapt to, and colonize either habitat.

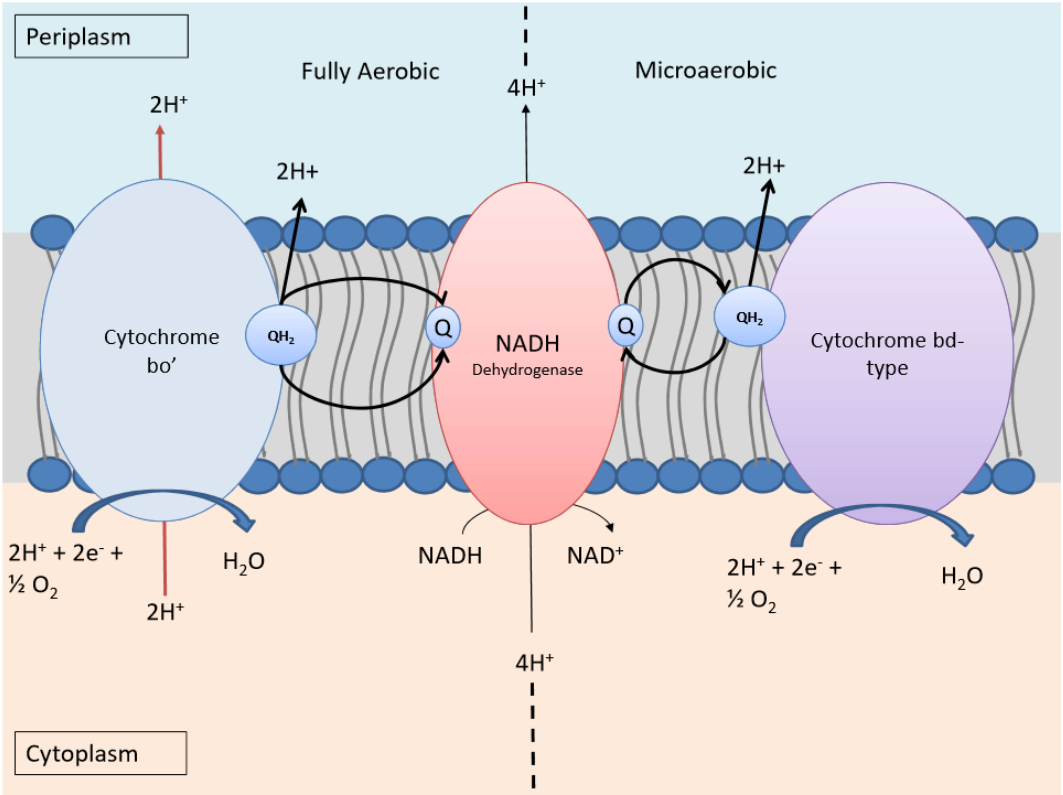

Figure 1.3 Selected components of the aerobic respiratory chain of E. coli. *In fully aerobic conditions, E. coli utilizes cytochrome bo' while in conditions of low oxygen E. coli has two different bd-type terminal oxidases that are expressed.*

An important process for niche colonization is the ability to generate a proton motive force across the inner membrane to provide energy to produce adenosine triphosphate (ATP) via oxidative phosphorylation. Aerobic respiration is the process of utilizing the electron transport chain (ETC) to successively pass electrons from electron donors, such as NADH, to dioxygen as the terminal

electron acceptor. During this process, energy is conserved as a proton gradient (Δψ) as protons accumulate in the periplasm (Figure 1.3). This gradient can then be used for processes such as ATP synthesis, which couples the transfer of protons with the phosphorylation of adenosine diphosphate (ADP) to make ATP. Aerobic respiration is characterized by having oxygen as the terminal electron acceptor, and *E. coli* has three terminal oxidase complexes that can catalyze oxygen reduction and couple this to generation of a proton motive force (Sousa, et al., 2012) and these are discussed in more detail below.

1.2.2. Respiratory oxidases of *E. coli*

The aerobic ETC pathway of *E. coli* has three known terminal oxidases: cytochrome *bo'*, cytochrome *bd*-I, and cytochrome *bd*-II. These oxidases combine the oxidation of ubiquinol with the reduction of oxygen to water (Figure 1.3) (Borisov, et al., 2011). Cytochromes *bd*-I and *bd*-II share sequence homology and have the same *b*-type and *d*-type heme cofactors (Sturr, et al., 1996), although they are expressed under different conditions. Cytochrome *bo'* is maximally expressed when oxygen levels exceed 20% (Tseng, et al., 1996) and is a heme-copper oxidase rather than *bd*-type (Borisov, et al., 2011) (Oost, et al., 1994).

1.2.2.1. Cytochrome *bo*'

The heme-copper oxidase family of cytochromes is one of the most diverse superfamilies of enzymes and encompasses cytochromes found all throughout the living world. This superfamily of enzymes relies on subunit I and its binuclear, or bimetallic, center where the reduction of oxygen occurs (Garcia-Horsmant, et al., 1994). *E. coli* possesses the heme-copper oxidase cytochrome *bo',* so named because it contains heme *b* and heme *o* (Oost, et al., 1994).

As the cytochrome reduces oxygen to water, it functions as a proton pump physically creating a proton motive force (Figure 1.3) to be tapped into for energetic purposes (Unden & Bongaerts, 1997). Cytochrome *bo'* is maximally expressed in fully oxic conditions suggesting it is primarily used by *E. coli* in

nonpathogenic stages of the cell. Expression is controlled by the global regulators Fnr and ArcA (Cotter, et al., 1990) (Cotter, et al., 1997).

Cytochrome *bo'* is comprised of four subunits encoded by the *cyoABCDE* operon (Nakamura, et al., 1997). Subunit I, encoded by *cyoB*, binds the low spin heme, heme *b,* and the binuclear center consisting of a Cu_B:heme *o* complex, which is the main site of oxygen reduction within cytochrome *bo'* (Pereira, et al., 2008) (Garcia-Horsmant, et al., 1994). Low spin (electrons fill the lower energy orbitals first, leaving minimal unpaired electrons) heme has been implicated as the driving force for transporting protons across the membrane in the mitochondrial heme-oxidase cytochrome c (Tsukihara *et al.* 2003); the low spin hemes present in cytochrome *bo'* may function in a similar manner. Subunit II, encoded by *cyoA*, is important in substrate binding and the transfer of electrons from ubiquinol to heme *b* in subunit I (Nakamura, et al., 1997). Subunits III and IV, encoded by *cyoC* and *cyoD* respectively, are suggested to be important for correct protein folding of subunit I (Nakamura, et al., 1997). The last gene in the operon, *cyoE*, is responsible for heme *o* synthesis (Nakamura, et al., 1997).

1.2.2.2. Cytochrome *bd*-type oxidases

Cytochromes belonging to the *bd*-family are quinol oxidases found throughout prokaryotes that couple the oxidation of ubiquinol to the formation of a proton gradient and reduction of oxygen to water. The *bd*-type oxidases of *E. coli*, cytochrome *bd*-I and *bd*-II, exhibit significant sequence homology and bind the same cofactors (Sturr, et al., 1996). Though cytochrome *bd*-I produces a proton gradient ($\Delta\psi$) via ubiquinol oxidation, it does not actively pump protons into the periplasm, separating from heme copper oxidases (Figure 1.3) (Borisov, et al., 2011). The lack of a proton pump makes it energetically less effective than cytochrome *bo'*: cytochrome *bd*-I has a H^+/e^- ratio of 1, and cytochrome *bo'* has a ratio of 2 (Unden & Bongaerts, 1997) (Borisov, et al., 2011) (Puustinen, et al., 1991). Early studies suggested that cytochrome *bd*-II did not contribute to the

proton gradient (Bekker, et al., 2009), although later it was shown to have a H^+/e^- ratio of 1 like cytochrome *bd*-I (Borisov, et al., 2011).

Cytochrome *bd*-I has been shown to be upregulated under microaerophilic conditions (Tseng, et al., 1996) and under conditions of nitrosative stress (Giuffre, et al., 2014) (Mason, et al., 2009), whereas cytochrome *bd*-II has been shown to be maximally expressed upon entry into stationary phase and during phosphate starvation (Atlung & Brondsted, 1994). Cytochrome *bd*-II is able to function in less aerobic conditions than cytochrome *bd*-I as the transcription is controlled by ArcA and AppY, not Fnr unlike cytochrome *bd*-I (Borisov, et al., 2011) (Atlung & Brondsted, 1994).

Two (b_{558} and b_{595}) of the three hemes present in cytochrome *bd* are protoheme IX groups while heme *d* is a chlorin molecule. Heme b_{558} is situated in subunit I (Green, et al., 1986) and is directly involved in quinol oxidation (Borisov, et al., 2011). It has been noted that both subunits are necessary for hemes b_{595} and *d* to assemble correctly suggesting the hemes are coordinated between them (Figure 1.4) (Newton & Gennis, 1991). The role of heme b_{595} still remains unclear, but together with heme *d*, the di-heme is suggested to be involved in oxygen reduction (Borisov, et al., 2011) (Borisov, et al., 2008). Further evidence suggesting the involvement of the di-heme in oxygen reducing is heme *d* high affinity to binding oxygen (Borisov, et al., 2011) making the *bd*-type oxidases ideal for microaerobic conditions.

Due to the involvement of *bd*-type cytochromes in virulence of pathogenic bacteria, and the role in growth and survival under a myriad of conditions, these oxidases have been viewed as a potential therapeutic target. Many inhibitory ligands like carbon monoxide, nitric oxide, and cyanide have been screened to this end (Meunier, et al., 1995) and have been found to bind to the active site readily (Borisov, et al., 2011) (Mason, et al., 2009) (Giuffre, et al., 2014), yet none have been successfully incorporated into a therapeutic. It is important to distinguish that though some ligands, e.g. nitric oxide, readily bind to the cytochrome *bd* active site, it also dissociates at a rate much faster than from the cytochrome *bo'* oxidase (Mason, et al., 2009).

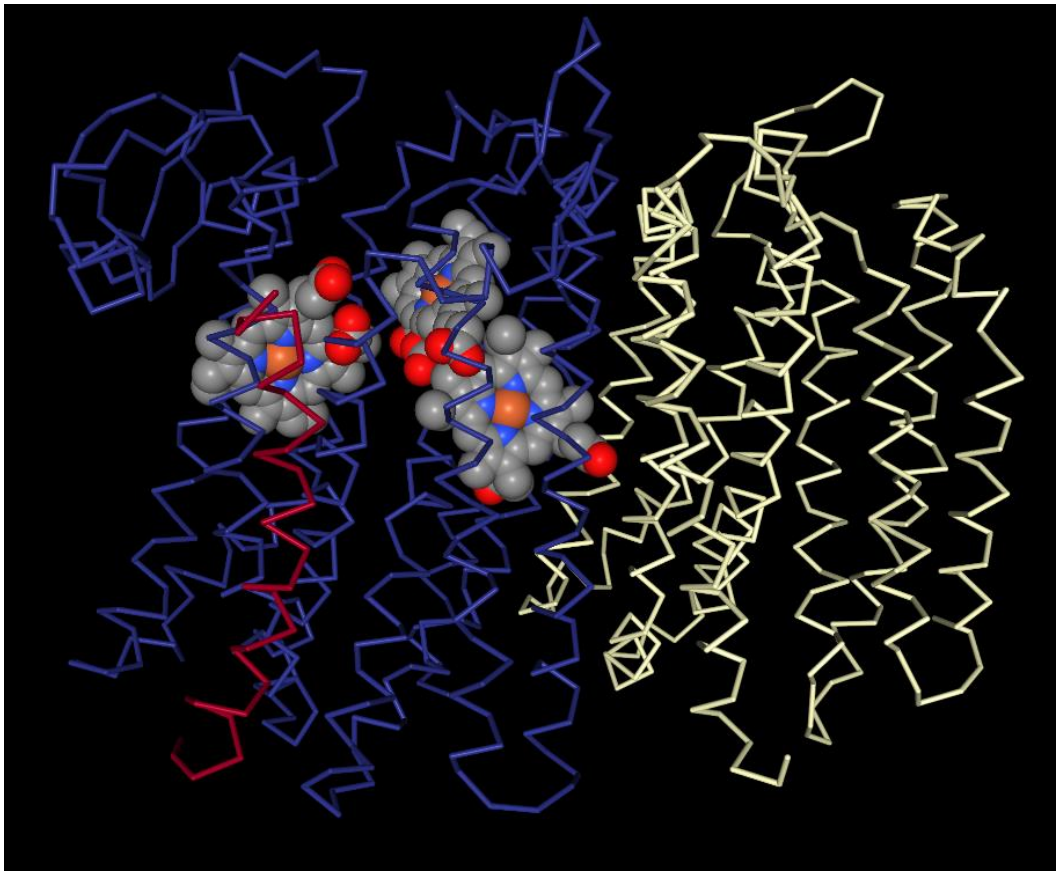

Figure 1.4 Model of the structure of cytochrome bd-type in Geobacillus thermodenitrificans*. Cytochrome bd in G. thermodenitificans and E. coli are nearly identical and the hemes are thought to reside in subunit I (Safarian, et al., 2016). The structure displayed is of G. thermodenitrificans with hemes displayed (protein data bank 5IR6); subunit I- blue, subunit II- yellow, single transmembrane helix - red.*

1.2.3. Respiration and antibiotics

Previous studies have reported a link between antibiotic treatment and elevated aerobic respiration in *E. coli* (Lobritz, et al., 2015) (Kohanski, et al., 2008) (Kohanski, et al., 2007). Though substantial work has surrounded the connection between antibiotics and cellular respiration, controversy exists on the mechanism. While one hypothesis suggests the oxidative burst from excess reactive oxygen species (ROS) leads to damaged lipids, DNA, and proteins, another hypothesis involves a mechanism via which certain antibiotics are imported more rapidly during elevated respiratory activity as uptake can be linked to the proton motive force (PMF).

The basis for ROS-mediated antibiotic cell death is visualized in Figure 1.5: As bactericidal antibiotics (specifically aminoglycosides, quinolones, and β-lactams) enter the cell and interact with their primary targets, the tricarboxylic acid (TCA)

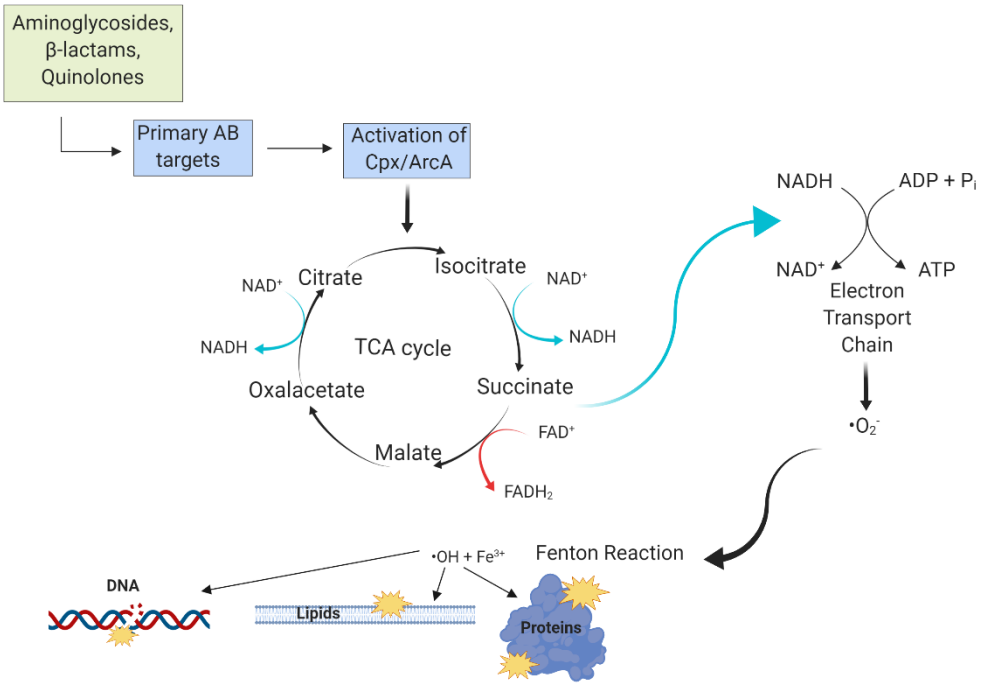

Figure 1.5 ROS-mediated cell death mechanism by bactericidal antibiotics. *A common mechanism for bactericidal antibiotics is described as the formation of reactive oxygen species ($^{\cdot}O_2^-$) from hyper activated ETC leading to cell damage. This is thought to be a main contributor to antibiotic-induced cell death. AB: Antibiotic. Adapted from Kohanski et al. (2010).*

cycle is stimulated in response to cellular stress (Cpx and Arc regulators). The increase in electron donors from the TCA cycle hyper stimulates the electron transport chain which in turn churns out more energy for the cell to utilize (Kohanski, et al., 2010). As a side effect to elevated respiratory activity, ROS such as superoxide and hydrogen peroxide are created (Imlay, 2003). When the ETC is hyper-activated the systems in place to detoxify ROS are unable to prevent the ROS from interfering with other processes (Zhao & Drlica, 2014), and the buildup of superoxide then can damage iron-sulfur centers releasing ferrous iron to be used in the Fenton reaction (Equation 1.1) which in turn release hydroxyl radicals that severely damage nucleotides, lipids, and proteins and lead to cell death (Kohanski, et al., 2010) (Kohanski, et al., 2007) (Dwyer, et al., 2014).

Equation 1.1 *Fenton reaction*

$$Fe^{2+} + H_2O_2 \rightarrow HO^{\cdot} + HO^{-} + Fe^{3+}$$

Though convincing research has been conducted to support the hypothesis above, numerous studies have cast doubt on this, as accurate measurement of ROS is technically difficult and reliable data is therefore hard to come by. HPF (hydroxyphenyl fluorescein), a common dye used in ROS studies, is not only preferentially oxidized by hydrogen peroxide but also by redox-active metals, making accurate determination of ROS very difficult (Liu & Imlay, 2013) (Keren, et al., 2013). Also, the longer *E. coli* is exposed to antibiotics the greater autofluorescence it produces (Renggli, et al., 2013), thus the more difficult a fluorescent signal is to detect and analyze (Van Acker & Coenye, 2017). Studies also report that bacteria lacking an ETC are highly susceptible to bactericidal antibiotics and bacteria with a noncyclic TCA cycle lack an increase in ROS production to contribute to cell death (Van Acker & Coenye, 2017). To add to this, *E. coli* was shown to have no difference in survival against a host of antibiotics under anaerobic and aerobic conditions (Keren, et al., 2013) (Liu & Imlay, 2013).

The other theory in which respiration influences antibiotic-mediated cell death corresponds to the uptake of the antibiotic. In accordance with the evidence

presented in the references above, research details the upregulation of TCA cycle and ETC genes when exposed to bactericidal antibiotics and documented resistance to the antibiotics in TCA cycle knockouts (Kohanski, et al., 2007). Yet instead of a ROS related pathway, some suggest this surge in ETC activity creates a larger PMF (Δψ), which promotes antibiotic uptake (aminoglycosides in particular): some aminoglycosides such as gentamicin have a positive charge; therefore, transport into the cell is thermodynamically favorable as the charge component of the PMF will be dissipated upon antibiotic entry (Ezraty, et al., 2013) (Taber, et al., 1987) (Farha, et al., 2018).

1.3. Immune Responses and Respiratory Inhibition of *E. coli*

1.3.1. Nitric oxide and the immune system

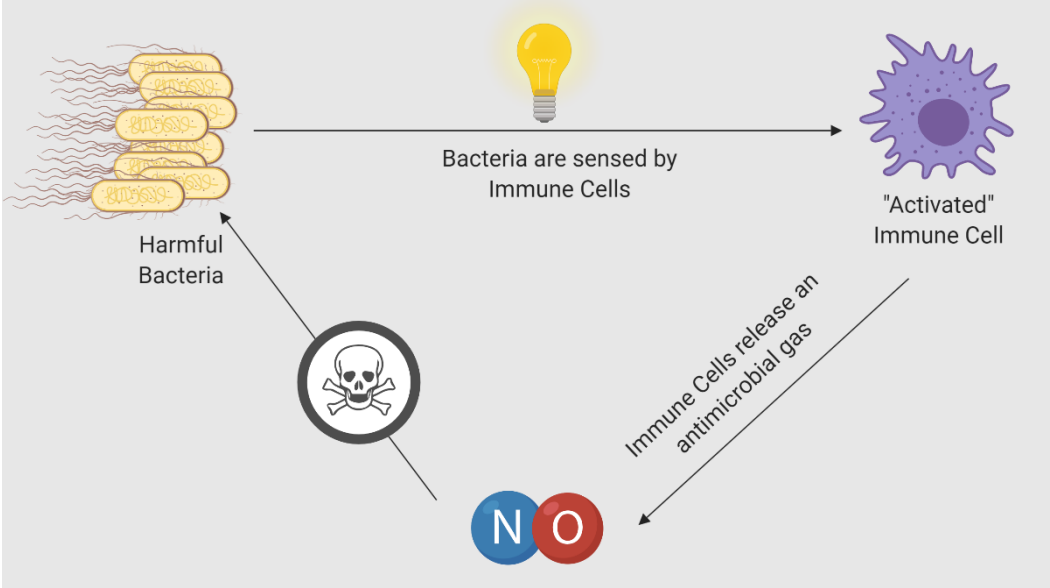

Figure 1.6 Nitric oxide (NO) released by immune cells is toxic to intracellular pathogens. *When pathogenic E. coli is sensed by activated macrophages, NO is released. NO reacts with reactive molecules within the cell to create highly toxic compounds that lead to cell death.*

Nitric Oxide (NO) is a free radical gas and within the human body it is known to function in circulation, nervous system, and the immune response (Roszer,

2012). Immune cells involved in the response to bacterial pathogens will produce NO to aid in their elimination (Figure 1.6) (Bogdan, 2001).

Synergistic relationships between NO and other free radicals are major contributors to its cytotoxicity. An important antimicrobial molecule is produced when NO encounters superoxide to make the reactive molecule peroxynitrite ($ONOO^-$). Strong oxidizing reactions of $ONOO^-$ allow it to disrupt DNA, lipids, thiol groups and proteins by binding tightly thus becoming much more cytotoxic than NO on its own (Bogdan, 2001) (MacMicking, et al., 1997) (Pacher, et al., 2007).

The potent bactericidal effects of NO and relatively low toxicity to mammalian cells highlight the potential use of NO-producing therapeutics to combat bacterial infections. Indeed, NO-donors have been used in several pharmacological studies (Feelisch, 1998) and many NO delivery molecules have been developed from such studies (Muscara & Wallace, 1999) (Nablo & Schoenfisch, 2003) (Hetrick, et al., 2008). However, one issue that will have to be considered is that bacteria often possess mechanisms of NO tolerance, so a detailed knowledge of these systems is necessary to properly assess the potential for NO as a therapeutic.

1.3.2. Nitric oxide and *E. coli*

Pathogenic *Escherichia coli* and nitric oxide are most likely to interact when the innate immune system is active and phagocytic cells (i.e. activated macrophages and neutrophils) are releasing NO into the environment (Figure 1.6) (Bogdan, 2001). *E. coli* may also encounter NO from nearby bacteria via bacterial homologues to mammalian nitric oxide synthases (iNOS) (Sudhamsu & Crane, 2009) (Crane, 2008) and/or from the byproducts of anaerobic respiration of other bacterial species (Jurtshuk, 1996). Hence, *E. coli* has evolved strategies to deal with this nitrosative stress. These strategies are summarized in Figure 1.7 and are described in detail below.

1.3.2.1. NO detoxifying enzymes

Periplasmic cytochrome *c* nitrite reductase (NrfA), when nitrate and/or nitrite is present, converts toxic NO into ammonium (Figure 1.7) (Wang &

Gunsalus, 2000) (Page, et al., 1990). It was shown that *E. coli* mutants deficient in NrfA were more sensitive to NO than the wild type in oxygen-limiting environments, suggesting NrfA plays an important role in NO detoxification under microaerobic and anaerobic conditions (Poock, et al., 2002).

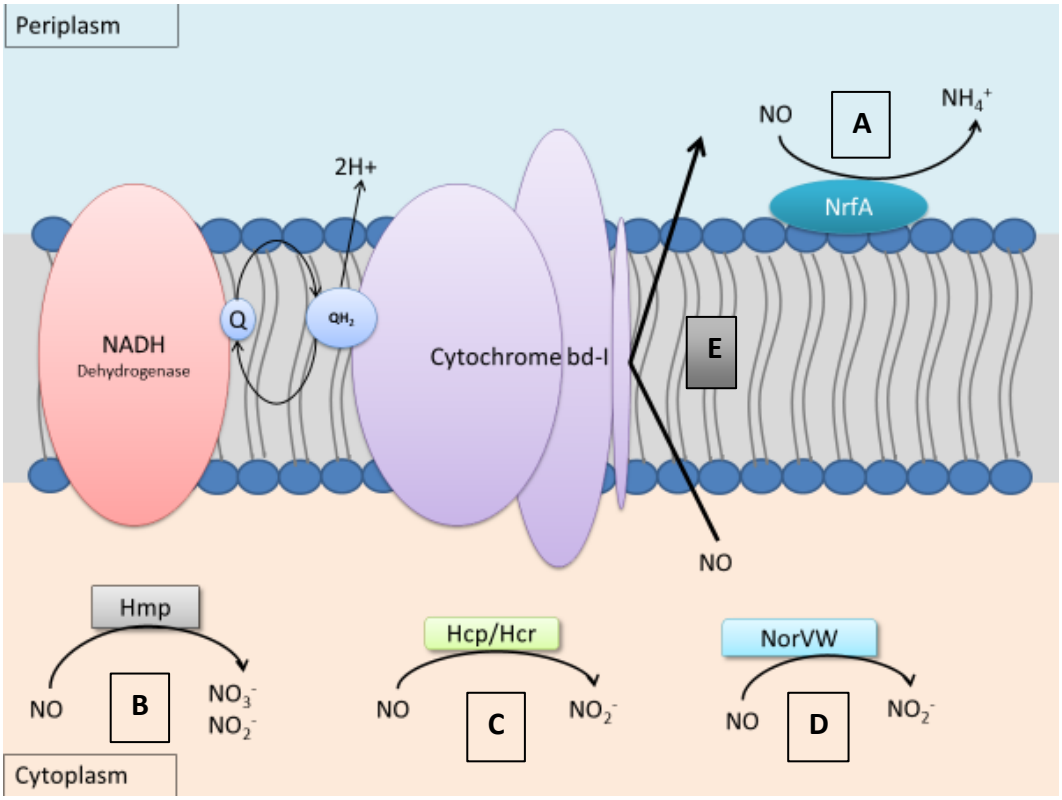

Figure 1.7 Schematic of various NO detoxifying proteins within E. coli. A) *NrfA sits on the membrane to convert NO into ammonium in oxygen-limiting conditions.* ***B)*** *Hmp, is the main contributor to NO scavenging in aerobic conditions and will convert NO into nitrite and nitrate.* ***C)*** *The hybrid cluster protein (Hcp) and its reductase (Hcr) convert NO into nitrite and is upregulated in low concentrations of NO.* ***D)*** *NorVW is the main NO scavenger in anaerobic conditions and converts NO to nitrite.* ***E)*** *Cytochrome bd-type oxidases have been shown to be NO-tolerant allowing respiration to continue under nitrosative stress.*

Flavohemoglobins are among the most widely distributed bacterial proteins and Hmp of *E. coli* is the best studied. Many sources have found substantial evidence for the upregulation of *hmp* in the presence of a nitric oxide donor (Poole, et al., 1996) (Hausladen, et al., 1998) (Poole & Hughes, 2000) (Membrillo-Hernandez, et al., 1999). Under aerobic conditions, Hmp will oxidize NO into mostly nitrate and some nitrite (Figure 1.7); however, under anaerobic conditions,

Hmp will use NADH to reduce NO into NO^- then N_2O (Hausladen, et al., 1998) (Kim, et al., 1999).

The flavorubredoxin protein NorV and the partner reductase NorW are important for the anaerobic detoxification of NO in *E. coli* (Gardner, et al., 2002). Multiple studies have shown an increase in transcription of *norVW* when various NO donors are present (Mukhopadhyay, et al., 2004) (Flatley, et al., 2005) (Pullan, et al., 2007). It was shown that while Hmp takes the leading role in detoxifying the cell of NO under aerobic conditions, NorVW dominates the detoxification process under anaerobic conditions (Gardner, et al., 2002) (Hutchings, et al., 2002) (Flatley, et al., 2005) (Poole, et al., 1996).

Among the most recently discovered systems in *E. coli* for the defense against nitrosative stress is the hybrid cluster protein (Hcp) and its accompanying hybrid cluster reductase (Hcr). Hcp was originally thought to be involved in oxidative stress functions (Almeida, et al., 2006), and was also described as a hydroxylamine reductase (Wolfe, et al., 2002). However, considerable evidence emerged that supported a role in the nitrosative stress response (Vine & Cole, 2011) (Filenko, et al., 2007) (van den Berg, et al., 2000) (Wang, et al., 2016). Hcp-Hcr seems be complementary to NorVW as Hcp is much more sensitive to the concentration of NO than NorVW is under anaerobic conditions. While Hcp is most active in scavenging NO at lower concentrations below 100 nM (Wang, et al., 2016), NorVW becomes most active when the cell is exposed to higher NO levels (Karlinsey, et al., 2012).

As briefly stated in section 1.2.2, respiratory oxidases will bind NO but this inhibitor will readily dissociate from NO-tolerant oxidases such as cytochrome *bd*-I of *E. coli* (Mason, et al., 2009). Previous studies have shown differential affinity towards NO and the possible benefits associated with the binding strategies employed. Cytochrome *bd*-I type has been experimentally shown to have high affinity for NO, but also high dissociation rates- compared to cytochrome *bo',*

suggesting that *bd*-I supports aerobic respiration in the presence of low levels of nitrosative stress (Figure 1.7) (Giuffre, et al., 2014) (Mason, et al., 2009).

1.4. Hypotheses and Research Strategies

As more novel therapeutics are needed to combat AMR, it is important to understand the underlying mechanism that allows pathogenic bacteria to escape the lethal action of antibiotics. As much debate over the mechanism which aerobic respiration can potentiate the toxic effects of aminoglycosides, the impact of the immune system upon this process has been largely overlooked. Hence, this was the chosen area of study for this MSc project. This project focused on four hypothesis and research strategies to understand the mechanism and is represented in Figure 1.8.

Hypothesis 1. NO will diminish the efficacy of the aminoglycoside gentamicin.

Research strategy 1: Viability assays in the presence of the NO-donor GSNO were chosen to investigate the effects of NO-mediated respiratory inhibition upon gentamicin-mediated killing.

Hypothesis 2: The *bd*-type oxidases will promote antibiotic-mediated killing in the presence of NO.

Research strategy 2: Strains with only one active oxidase were constructed to be used in viability assays in the presence of GSNO to investigate to effects of NO-mediated respiratory inhibition upon each oxidase and gentamicin-mediated killing.

Hypothesis 3: Gentamicin will elevate aerobic respiratory rates in *E. coli*.

Research strategy 2: Oxygen consumption rates of wild type and newly constructed mutants were used to investigate the effects gentamicin has upon respiration.

Hypothesis 4: Gentamicin will elevate ROS production in *E. coli*, and NO will counteract this.

Research strategy 4: Precise ROS measurements were gathered in the presence of GSNO and gentamicin to investigate the effects of NO-mediated respiratory inhibition upon gentamicin-mediated ROS generation.

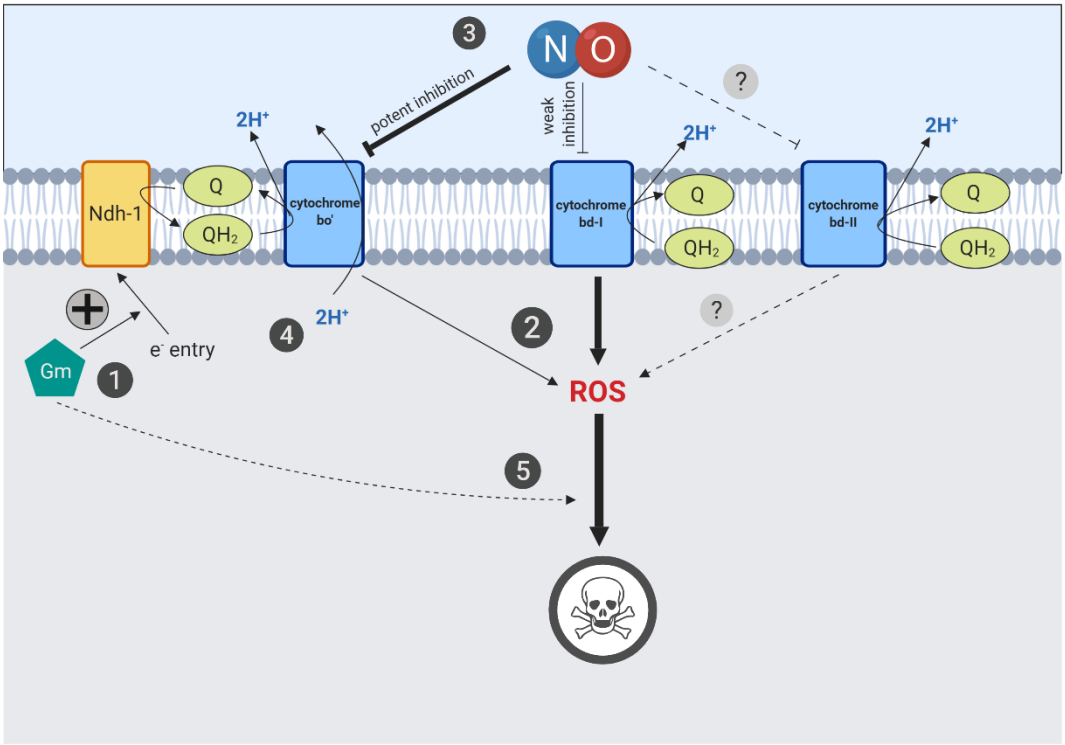

Figure 1.8 Differential contribution of the E. coli terminal oxidases to ROS and pmf generation in the presence of NO may affect antibiotic susceptibility. 1) *Gentamicin increases e^- entry into the ETC which stimulates respiration.* ***2)*** *Increased respiration promotes ROS and pmf generation.* ***3)*** *NO differentially inhibits the terminal oxidases affecting their contribution of ROS and pmf generation.* ***4)*** *Cytochrome bo' is the only oxidase that acts a proton pump while bd-I and bd-II contributes minimally to pmf; in the presence of NO pmf generation is dependent on the level of inhibition.* ***5)*** *Gentamicin-mediated ROS production is hypothesized to be the primary cause for cell death by aminoglycosides while the primary mode of action plays a minor part in cell death.*

Chapter 2

Materials and Methods

2.1. Bacteriological Methods

2.1.1. Bacterial strains and plasmids

The bacterial strains and plasmids used and created are listed below in Table 2.1 and Table 2.2, respectively. All bacterial strains utilized during this project are derivatives of *E. coli* clonal group ST131 strain EC958. Plasmid maps are shown in Figure 2.1

Table 2.1 *List of bacterial strains (all derived from E. coli EC958)*

Strain	Strain Description	Plasmid	Antibiotic Resistance	Reference
MS10	WT	-	ESBL	Lau, et al., 2008
MS11	WT	pKOBEG_Gm	ESBL, Gm, Ap	Shepherd laboratory
MS16	*cydAB::*Cm^R	-	ESBL, Cm	Shepherd *et al.*, 2016
MS107	WT	pCP20_Gm	ESBL, Gm, Tet	Shepherd *et al.*, 2016
MS506	*cyoA::*Cm^R	-	ESBL, Cm	Claudia Ribeiro, Shepherd laboratory
MS605	*appCB::*Cm^R	pKOBEG_Gm	ESBL, Gm, Cm	Louis Holmes, Shepherd laboratory
MS613	*appCB::*Cm^R	-	ESBL, Cm	This work
MS614	*cydAB*	-	ESBL	Calum Webster, Shepherd laboratory
MS623	*cyoA*	pKOBEG_Gm	ESBL, Gm	This work
MS625	*cydAB*	pKOBEG_Gm	ESBL, Gm	Calum Webster, Shepherd laboratory
MS628	*cyoA appCB::*Cm^R	-	ESBL, Cm	This work
MS629	*cydAB appCB::*Cm^R	-	ESBL, Cm	This work
MS630	*cydAB cyoA::*Cm^R	-	ESBL, Cm	This work

Table 2.2 *List of plasmids used*

Plasmid	Plasmid Description	Antibiotic Resistance	Parent Strain
pCP20-Gent	10,030 bp; Expression of Flippase; Temperature sensitive (ts) replicon	Gentamicin, Ampicillin	MS107
pKOBEG-Gent	8,264 bp; Expression of λ-red machinery	Gentamicin, Tetracycline	MS11

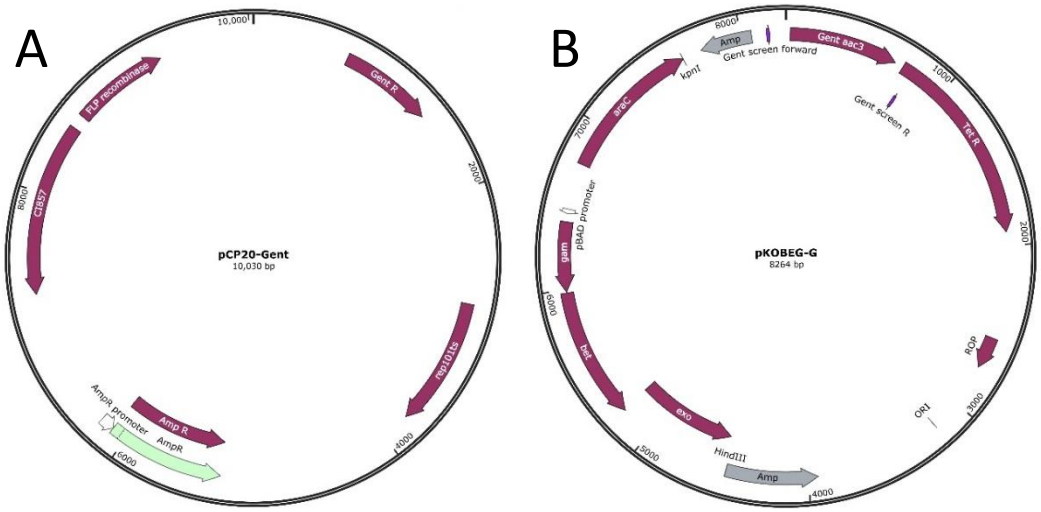

Figure 2.1 Map of plasmids used in this study. ***A)*** *Map of pCP20_Gm plasmid.* ***B)*** *Map of pKOBEG_Gm plasmid.*

2.1.2. Oligonucleotides

All oligonucleotides utilized are listed in Table 2.3. Oligonucleotides designed for this body of work were synthesized by Integrated DNA Technologies.

Table 2.3 *List of oligonucleotides used*

Primer Number	Name	5' – 3' Sequence	Use	Direction
238	cyoA_Sc_fw	GTCAACGGAGGTCAGCCACT	Screen presence or absence of *cyoA* gene	Forward
260	cyoA_Sc_rev2	CGCCCTTTTGCAACAGCTTC	Screen presence or absence of *cyoA* gene	Reverse
271	cyoA_EC_fw	TTCGCCCGCAGAGGCAAGGG	For screening of cyoA locus in EC958	Forward
272	cyoA_EC_rev	TGCCCGCCCAAACTCCTTCT	For screening of cyoA locus in EC958	Reverse
336	appCsc_F	GTGCTGGCAGCGCCAGAAGA	Screen presence or absence of *appCB* gene	Forward
337	appBsc_R	CAGAAGAGATAAGAATGGGA	Screen presence or absence of *appCB* gene	Reverse
392	AppCB_500_F	TCGTCACTTTATCAATACGCTTCT	Amplification of the chloramphenicol cassette for replacement of the *appCB* gene. Amplifies 500bp overhang from a Δ*appCB* strain	Forward
393	AppCB_500_R	AGTTTGATTGCGGGAAATTAAGCA	Amplification of the chloramphenicol cassette for replacement of the *appCB* gene. Amplifies 500bp overhang from a Δ*appCB* strain	Reverse
394	cydAB_F_600bp	GTGACGGATTTACAGTACGTTGCT	Amplification of the chloramphenicol cassette for replacement of the *cydAB* gene. Amplifies 500bp overhang from a Δ*cydAB* strain	Forward
397	cyoA_F_500_New	CGAGAGAAACGTTAACCAGAATCA	Amplification of the chloramphenicol cassette for replacement of the *cyoA* gene. Amplifies 500bp overhang from a Δ*cyoA* strain	Forward
398	cyoA_R_500_New	GTTTGCTGGATTATCTGGCGCTAC	Amplification of the chloramphenicol cassette for replacement of the *cyoA* gene. Amplifies 500bp overhang from a Δ*cyoA* strain	Reverse
417	CydAB_R_500bp_new	CTGCTACTATACGCGCGCGATTGA	Amplification of the chloramphenicol cassette for replacement of the *cydAB* gene. Amplifies 500bp overhang from a Δ*cydAB* strain	Reverse

420	AppCB_200_F	GGCATTTACGCTGTACGGAC	To screen Cm cassette insertion into AppCB locus of EC958 - Binds 200bp upstream of AppC	Forward
421	AppCB_200_R	TGGCGTTGGTAATGTCCGAG	To screen Cm cassette insertion into AppCB locus of EC958 - Binds 200bp downstream of AppB	Reverse
422	CmR_Sc1	CATTCATCAGGCGGGCAAGAATGTG	To screen Cm cassette insertion - binds in the middle of Cm gene	Forward
426	cyoA_Sc_revN	CCTTCTGCACTTCCCTTTCG	200bp overlap screening primer for *cyoA* deletion in EC958 ST131	Reverse

2.1.3. Chemicals

Chemicals were purchased from Sigma unless stated otherwise. Nutrient agar, tryptone, and yeast extract were purchased from Oxoid. The Total Reactive Oxygen Species (ROS) Assay Kit 520 nm was purchased from ThermoFisher Scientific. Deionized and Milli-Q (MQ) water were used throughout. Reagents that required sterilization were autoclaved at 121°C, 15 psi (pounds of force per square inch) for 15 min; alternatively, filter sterilization was utilized using Millipore filters with 0.22 µm pore size.

2.1.4. Media and buffer solutions

2.1.4.1. Luria-Bertani media

250 mL of Luria-Bertani (LB) media contained 2.5 g of NaCl, 2.5 g of tryptone, and 1.25 g of yeast extract. Additionally, 3.75 g of nutrient agar was added when solid media was needed. The media was autoclaved for sterilization.

2.1.4.2. Super optimal broth with catabolite repression (SOC) media

SOC broth was made by adding 10 g tryptone, 2.5 g yeast extract, 0.292 g NaCl, and 0.093 g KCl to 485 mL of MQ water. The solution was autoclaved. When the broth was cooled to below 60°C, 5 mL of sterile 2M Mg^{2+} and 10 mL of sterile 1M glucose stock was added.

2.1.4.3. Super optimal broth (SOB) media

SOB media was prepared as for SOC media without the addition of glucose.

2.1.4.4. M9 minimal media

One liter of M9 minimal media was made by combining 200 mL 5X M9 salts, 2 mL 1M $MgSO_4$, 100 µL 1M $CaCl_2$, 20 mL 20% (w/v) glucose, 50 mL 2% (w/v) casein hydrolysate, and 777 mL autoclaved deionized water.

5X M9 salts consisted of 80.24 g sodium phosphate dibasic dihydrate ($Na_2HPO_2{\cdot}2H_2O$), 15 g potassium phosphate monobasic (KH_2PO_4), 2.5 g NaCl, and 5 g

NH_4Cl added to 1 L of deionized water. This solution was thoroughly mixed then autoclaved for sterilization.

2.1.4.5. Phosphate-buffered saline (PBS)

1X PBS solution was made by adding one tablet (oxiod dulbecco A) to 100 mL deionized water. The solution was stirred until the tablet was completely dissolved then autoclaved for sterilization.

2.1.5. Media supplements

Ampicillin powder was dissolved in deionized water to produce a stock concentration of 125 mg/mL; the final concentration in supplemented media was 125 µg/mL. Chloramphenicol powder was dissolved in 100% ethanol to produce a stock concentration of 34 mg/mL; the final concentration in media was 25 µg/mL. Gentamicin powder was dissolved in deionized water to produce a stock concentration of 30 mg/mL; the final concentration in supplemented media was 30 µg/mL. All stocks were filter sterilized before use.

2.1.6. Bacterial growth conditions

Unless otherwise stated, 10 mL starter cultures were inoculated from a single colony and grown overnight at 37 °C and 180 rpm in LB broth. Fresh media was inoculated with 1% starter culture (v/v). A New Brunswick™ Innova® 3100 model water bath was used to grow liquid cultures.

2.1.6.1. Optical density of *E. coli* culture

The cell density of *E. coli* cultures was measured using a Cary 60 UV-vis spectrophotometer (Agilent Technologies) at 600 nm.

2.1.6.2. Glycerol stocks of *E. coli* strains

When a new strain was confirmed or an old strain was replaced, glycerol stocks were made by adding 500 µL 50% (v/v) glycerol to 500 µL overnight starter culture in a sterile cryotube. This cryotube was appropriately labeled and stored at -80°C.

2.1.7. Gentamicin viability assay

2.1.7.1. S-Nitrosoglutathione (GSNO) preparation

GSNO was used as the exogenous source of nitric oxide. GSNO was made as previously described (Hart, 1985). Briefly, in a foil-wrapped 100 mL flask on ice, 3.08 g reduced glutathione, 0.69 g of sodium nitrite ($NaNO_2$), and 0.83 mL 12.1 M HCl were added to 18 mL deionized water. After 40 min of stirring on ice, 20 mL of acetone was added to the red solution and stirred on ice for an additional 10 min. The red/pink precipitate was collected via vacuum filtration then washed with 2 mL ice-cold water five times, 10 mL acetone three times, and finally 10 mL ether three times. The red/pink gummy product was placed into a foil wrapped desiccator attached to a vacuum and left to dry overnight. The dry powder was placed in a foil wrapped falcon tube and placed in the -80°C freezer for no longer than one month.

GSNO was dissolved in water immediately before use. The concentration of the filter sterilized solution was determined by diluting 1:20 in deionized water in a cuvette and OD_{545} was measured. The extinction coefficient (ε_{545}) 15.9 $M^{-1}cm^{-1}$ was used for quantification (Mohr, et al., 1996).

2.1.7.2. Viability assays

10 mL of M9 minimal medium was inoculated with an overnight starter culture of each strain. The culture was grown to an OD_{600} of at least 0.3. Once reached, the cultures were diluted to an OD_{600} of 0.125 in 5 mL M9 medium or 5 mL M9 medium containing 15 mM GSNO. Both cultures were statically incubated at 37°C for 30 min. The pre-exposed cultures were then exposed to various concentrations of gentamicin and statically incubated at 37°C for an additional 90 min. Serial dilutions were performed in 1X PBS and 5 µL was plated in triplicate on LB agar (Figure A.1). The plates were incubated at 37°C overnight and calculations to determine CFU/mL were conducted. Concentrations of gentamicin used (µg/mL): 0.1, 0.5, 1, 5, 10, 50, 100, 250, 500, 1000.

Two controls without the addition of gentamicin were averaged then used as the base value for data normalization for a '100% survival' control. Percent survival data for each technical repeat was plotted against the concentration of antibiotic. Once plotted, IC_{90} was calculated using GraphPad Prism 6. IC_{90} of 2 biological and at least 3 technical repeats were averaged, and standard deviation was used for error bars.

2.1.8. Measurement of aerobic respiration rates using an oxygen electrode

10 mL of freshly made M9 was inoculated with 100 µL starter culture in a 50 mL flask. The culture was incubated in a shaking water bath at 37°C and 180 rpm until an OD_{600} of 0.6. Once reached, cells were pelleted and kept on ice until ready to use.

To prepare the electrode (Rank Brothers), the water bath and connected pump was turned on to flow throughout the chamber while the chamber was filled with deionized water, stir bar turned on, and the plunger left off overnight. On the day of the experiment, the electrode was calibrated first with deionized water then M9 media.

Three biological repeats were conducted for each strain tested. Pelleted cells were resuspended in M9 to achieve a final OD_{600} of 2; cells were diluted by 10-fold to record OD_{600}. Either M9 or M9 with 15 mM GSNO (section 2.1.7.1) was added to the chamber and was left to equilibrate. Once the trace had settled, a baseline signal was recorded for 5 min. Cells were added to a final concentration of OD_{600} = 0.1 into both chambers simultaneously and left for 30 min with the plunger off. After the pre-exposure period, a final concentration of 100 µg/mL gentamicin or an equal value of sterile water was added to the chamber and the plunger was immediately placed onto the chamber to eliminate air bubbles. Oxygen consumption was recorded for an additional 30 min.

Oxygen consumption rates (OCR) were measured at least 100 seconds after gentamicin treatment at the fastest rate on consumption. The electrode used

exports oxygen diffusion as voltage; thus, concentration of oxygen was determined using the saturating O_2 concentration of 200 µM (Equation 2.1)

Equation 2.1 *Conversion for oxygen concentration. V= output voltage; media saturating concentration of oxygen= 200 µM; V_{max} = highest output voltage.*

$$[O_2] = V \times (\frac{200\mu M}{V_{max}})$$

2.1.9. Reactive oxygen species Assay

2.1.9.1. Method development

Reactive oxygen species (ROS) are fleeting and are difficult to accurately measure. There is no standardized method to measure ROS, therefore careful experiment design was pertinent to ensure accurate and reliable results were achieved. The assay was designed to mirror the cell survival assay (section 2.1.7.2) in which cells were left to incubate with antibiotic for a maximum of 90 minutes after pre-exposure to GSNO. It has been shown *E. coli* will naturally grow in autofluorescence the longer it is exposed to antibiotic (Renggli, et al., 2013). The ROS dye used from the Thermo Fisher Total Reactive Oxygen Species Assay Kit 520 nm (catalog number: 88-5930-74) detects NO as well as ROS; therefore, meticulous controls were gathered to ensure accurate results. A 4-gate analytical scheme adapted from McBee, et al. (2017) was used to aid in method development (Figure 2.3A).

A BD FACSJAZZ™ flow cytometer was used to analyze samples for fluorescent signals. In each sample, at least 100,000 events were captured. The four gates used to determine activated ROS dye were: 1) cell size (single cell gate), 2) intact DNA (dapi gate), 3) elimination of background fluorescence (autofluorescence gate), and 4) ROS-activated dye (ros hi gate) (Figure 2.3). The first gate, cell size, was determined by the forward-scatter (FSC; measures size of a particle) and side-scatter (SSC; measures internal complexity). Size was determined by eliminating doublets and assessing where most cells resided for each time point. All events

that passed the first gate were screened by the second gate- intact DNA. This gate was used ensure only intact cells were analyzed. The third gate was used to eliminate fluorescence originating in places other than activated dye (i.e. media and autofluorescence). Gentamicin-treated, DAPI-only dyed cells were used at each time point to account for autofluorescence. After background fluorescence was accounted, cells that exhibited fluorescence above a basal rate were collected. Untreated ROS- and DAPI-dyed cells were used at each time point to determine basal rate and accurately place this gate. Cells above this last gate were determined to have metabolically activated the ROS dye.

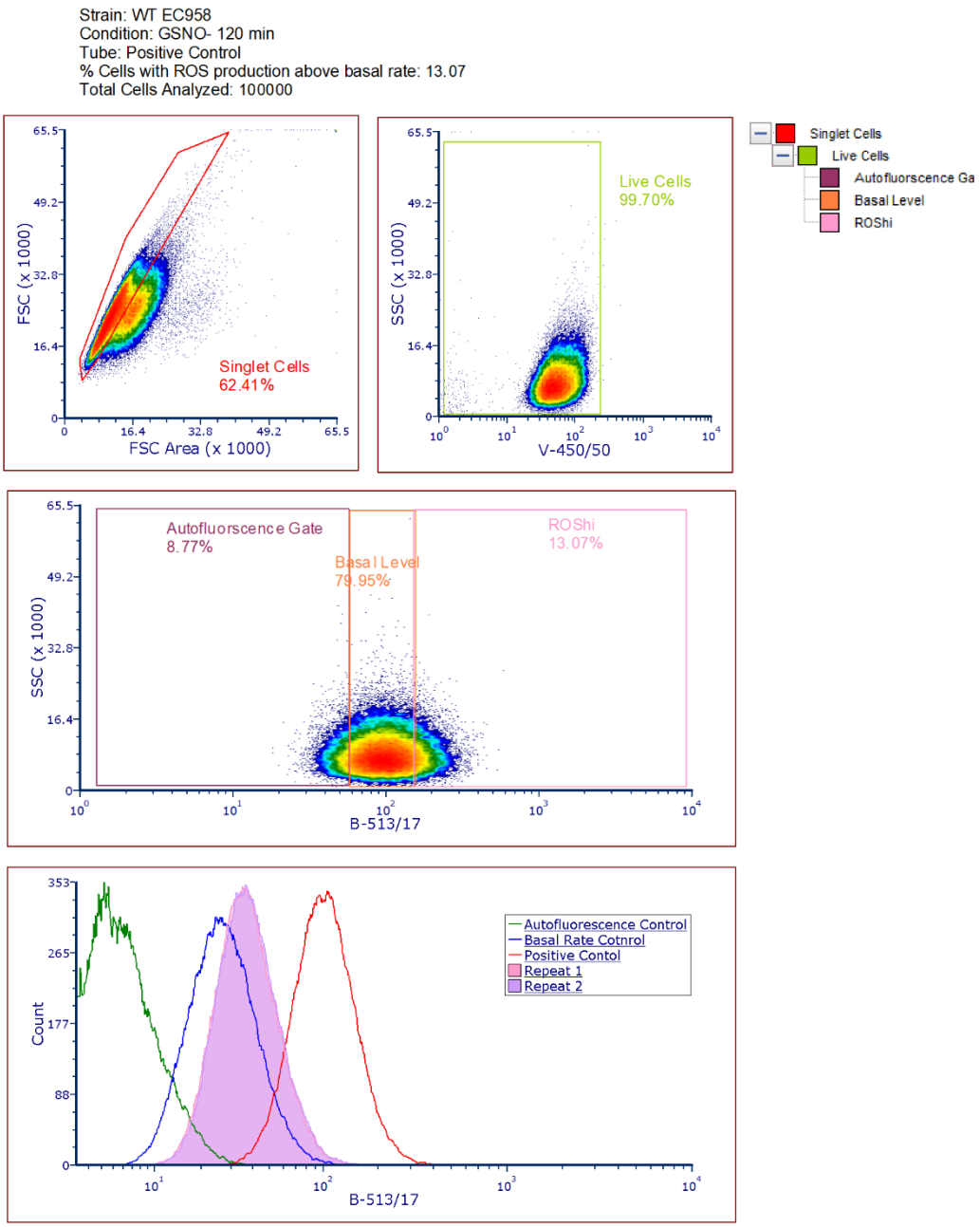

Figure 2.2 A robust gating procedure was used to analyze ROS production in E. coli. *A representative plot layout to determine gates is shown using the GSNO positive control at the 120 minute time point. The first gate (singlet gate) eliminated doublets, aggregates, and debris. The subsequent gate (live cells) was used to ensure only cells with intact membranes were analyzed. Multiple controls were used to ensure the ROShi gate was properly placed. Cells within the ROShi gate were used to analysis. This histogram displays the controls used at the time point along with the experimental data. Data was analyzed utilizing FCS Express 7.*

2.1.9.2. Protocol

ROS was identified using a DCFA (2', 7'-Dichlorofluorescin Diacetate) analog purchased in the Total Reactive Oxygen Species Assay Kit 520 nm from ThermoFisher. Ten mL of fresh M9 minimal media was inoculated with 100 µL overnight starter culture in duplicate for the strain analyzed and incubated at 37°C and 180 rpm. Once early log phase was reached, OD600 0.3, cells were placed on ice to prevent further growth. Cells were then diluted using M9 minimal media or M9 minimal media with the addition of 15 mM GSNO to an OD600 0.125. 500 µL of diluted cells were dyed with 0.5 µL of ROS dye then 200 µL of the ROS-dyed culture was aliquoted into a sterile well to incubate at 37°C for 30 minutes. Three time points were chosen to measure ROS: immediately prior to gentamicin treatment, 30 minutes post gentamicin treatment, and 90 minutes post gentamicin treatment. At each time point two technical repeats of 20 µL were gathered for measurement from each duplicate. After the first time point (before gentamicin treatment) samples were gathered, gentamicin was added to the cultures at a final concentration of 100 µg/mL. The cultures were thoroughly mixed then placed back into the incubator at 37°C until samples were sampled at the additional time points.

Once the samples were collected, they were diluted, fixed, and DNA-stained prior to measurement. A solution of 25 µg/mL DAPI (4', 6-diamidino-2-phenylindole) in 4% paraformaldehyde (PFA) in PBS (w/v) was used to fix and stain the DNA of the cells. The 20 µL samples were diluted in 180 µL of PBS. 50 µL of the DAPI-PFA-PBS solution was added to the sample and left at room temperature for at least 10 minutes but no more than 2 hours. Once fixed and stained, the samples were analyzed using the BD FACSJAZZ as explained above (Section 2.1.9.1).

2.1.9.3. Data analysis

Careful measurements and controls were used to ensure accuracy of ROS production. Cells that were selected in the final gate were determined to have ROS production above the basal rate of ROS production. Basal rate was determined by measuring the ROS production in untreated wild type *E. coli* cells. The percentage

of total cells passing from gate 3 that qualified for gate 4 were used in analysis (Figure 2.3). Statistical analysis was conducted using GraphPad Prism 6.

2.2. Genetic Methods

2.2.1. Plasmid DNA isolation

Two plasmids were used during this work as listed in Table 2.2. The QIAprep Spin Miniprep Kit (QIAGEN) was used to isolate plasmids from parent strains using manufacture instructions. Sterile deionized water was used to elute the plasmids. Miniprepped plasmid DNA were frozen until needed.

2.2.2. Polymerase chain reaction (PCR)

The PCR reactions conducted within this body of work were exclusively colony PCR. A typical PCR reaction would contain 25 µL Q5® High-Fidelity 2X Master Mix (New England Biolabs) or 2x PCRBIO Taq Mix Red (PCRBiosystems), 21 µL sterile MQ water, 300 nM of each primer, and 1.0 µL of resuspended colony. The PCR tubes were then placed in a thermocycler programmed with: one cycle at 94°C for 5 minutes, 30-35 cycles at 94°C for 15 seconds, 50-65°C (depending on primer T_m) for 30 seconds, and 72°C for 4-5 minutes, one cycle at 72°C for 5 minutes, and finally a hold at 10°C until removed from the thermocycler.

2.2.3. DNA electrophoresis

30 mL 1% (w/v) agarose gels with 0.5 µg/mL ethidium bromide (Sigma) added were prepared with 1X TAE buffer and used for DNA electrophoresis. The typical conditions set were 80V, 150 mA, for 40-60 minutes. 5 µL of DNA was mixed with 1 µL of Blue/Orange 6X loading dye (Promega) then added to gel wells unless otherwise stated. 5 µL of a 1 kb DNA ladder (Promega) or 5 µL of a 1 kb Hyperladder™ (Bioline) was loaded in the first well to determine size of DNA fragments. Pictures of the agarose gels were captured in a UV box.

Chapter 3

Results

3.1. Creation of Respiratory Mutants

In order to address the hypotheses outlined in Section 1.4, it was necessary to create a suite of *E. coli* strains that encode a single respiratory oxidase. Strains expressing 'cytochrome *bd*-I only' and 'cytochrome *bd*-II only' were created within this body of work; the strain expressing 'cytochrome *bo'* only' was provided by Calum Webster in the Shepherd laboratory.

3.1.1. An optimized protocol

E. coli possesses three known respiratory oxidases: cytochrome *bo'*, *bd*-I, and *bd*-II. Single knockout mutants of each oxidase existed prior to beginning this research (Table 2.1). Three new mutants strains expressing only one oxidase were generated using flippase-FRT (Flp-FRT) recombination and optimized lambda-Red (λ-Red) recombination technology as described in Datsenko & Wanner (2000).

The three single mutant strains possessed an antibiotic (chloramphenicol) resistance marker (Cm^R) in place of the excised oxidase gene. These loci were first amplified with at least 500 bp overhangs on either side of the cassette for subsequent λ-Red recombination. The Cm^R cassette was then excised from each single KO mutant using Flp-FRT recombination that target the FRT sites that flank the Cm^R cassettes. The single mutants without antibiotic markers were then used as the base organism to create double knockout strains via λ-Red recombination.

3.1.1.1. Amplification of the chloramphenicol cassette

To begin the creation of the double mutants, amplification of Cm^R cassettes from the existing mutants was necessary. A large region of homology up- and

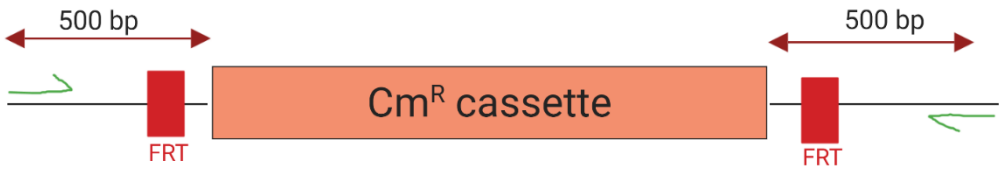

Figure 3.1 Cm cassettes in place of excised oxidases were amplified. *CmR cassettes in place the locus of a cytochrome gene was amplified with primers at least 500 bp away to ensure a large homology region to utilize during λ-Red recombination.*

downstream of the Cm^R cassette was essential for a successful λ-Red experiment (Figure 3.1).

The Cm^R cassette in the MS16 strain, a mutant with Cm^R in place of *cydAB*, was amplified using primers (Table 2.3) that bound at least 500 bp up- (#394) and downstream (#417) of the gene locus (Figure A.1); this cassette was later used to replace the *cydAB* gene to create a double knockout mutant. The Cm^R cassette in the MS506 strain, Cm^R inserted in place of *cyoA*, was amplified with primers that bound at least 500 bp up- (#397) and downstream (#398) of the gene locus (Figure A.2); this isolated cassette was used to replace the *cyoA* gene in a double knockout mutant. The Cm^R cassette in the MS605 strain, Cm^R inserted in place of *appCB*, was amplified using primers that bound at least 500 bp up- (#392) and downstream (#393) of the gene locus (Figure A.2); this Cm^R cassette was used in subsequent experiments to create a double knockout mutant.

3.1.1.2. Flp-FRT recombination

Once the Cm^R cassettes were amplified from the single mutant strains, the present Cm^R cassette required removal. An FRT (flippase recognition target) site was located on either side of the Cm^R gene. The recombinase flippase (Flp), encoded on the plasmid pCP20_Gm (Figure 2.1A), was used to excise the Cm^R cassette from the strains by allowing the cultures to incubate at 28°C and 180 rpm for 24 hours, changing to fresh media every 12 hours.

3.1.1.3. λ-Red recombination

The last step in the creation of double knockout mutants was to insert the Cm^R cassette with the large regions of homology in place of the appropriate gene. After initial failures (data not shown) to incorporate the Cm^R cassette into the single mutant strains, a systematic approach was taken to optimize the protocol. The λ-Red machinery (Exo, Gam, and Beta proteins) located on the pKOBEG_Gm plasmid (Figure 2.1B) that facilitated recombination with chromosomal DNA were under control of an *araC* promoter. The *araC* promoter was found to be optimally expressed when L-arabinose was the sole carbon source in M9 minimal media

(Guzman, et al., 1995) rather than SOB media as described in (Datsenko and Wanner 2000).

To express the λ-Red proteins and perform the successful recombination experiment, 500 µL of starter culture was made electrocompetent by inoculating into 50 mL of M9 minimal media (no glucose) supplemented with 20 mM L-arabinose and 30 µg/mL gentamicin added. The culture was incubated in a 250 mL flask at 28°C and 180 rpm until an OD_{600} of 0.3-0.6 was reached. Once reached, cells were transferred to an ice-cold 50 mL Falcon tube and pelleted at 8000 *x g*, 4°C, for 10 minutes. The pellet was resuspended in 25 mL of ice-cold 10% (v/v) glycerol then spun at 4000 *x g*, 4°C, for an additional 10 minutes. This pellet was resuspended in 5 mL ice-cold 10% (v/v) glycerol then spun at the same conditions as before. The last resuspension was in 200 µL of ice-cold 10% (v/v) glycerol and the cells were either frozen or immediately used to electroporate the Cm^R cassette into.

Electrocompetent cells and the appropriate Cm^R cassette or MQ water (control) were added to a chilled electro-cuvette then tapped gently to mix. The cuvette was thoroughly dried then placed in a Bio-Rad electroporator with the following programmed conditions: 2450 V, 200 Ω resistance, 25 µF capacitance. The time-constant of the electroporation was recorded and 1 mL of prewarmed (37°C) SOC was immediately added to the cuvette then transferred to a sterile microcentrifuge tube. The cells were left to recover at 37°C and 180 rpm for 2 hours. After recovery time, the cells were pelleted at 5000 rpm for 5 mins. 100 µL of cells were resuspended in remaining supernatant then plated onto prewarmed LB agar plates containing chloramphenicol. Plates were incubated for a least overnight at 37°C and up to 5 days. When chloramphenicol resistant colonies appeared, they were screened via colony PCR to ensure the Cm^R cassette was inserted in the correct locus using the screening primers listed in Table 2.3. Once confirmation was adequate using colony PCR the colonies were sequenced by GENEWIZ®.

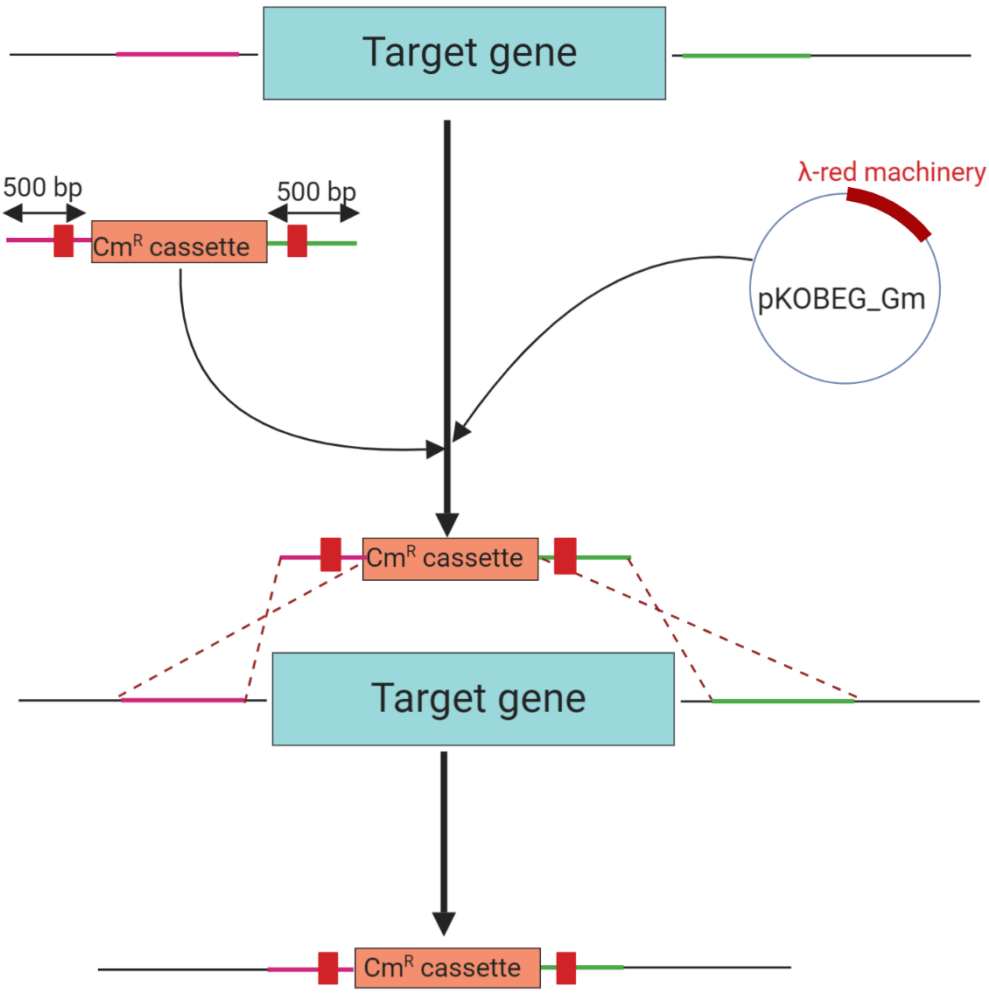

Figure 3.2 λ-Red recombination was used to replace an oxidase gene with the chloramphenicol cassette. *The amplified CmR cassette possesses at least 500 bp regions of homology with either side of the target oxidase. λ-Red proteins utilize the homology regions to excise the target oxidase gene and insert the Cm^R cassette.*

3.1.2. Engineering a 'cytochrome *bd*-I only' strain

The strategy in achieving this mutant was to begin with a single KO mutant still containing the *cydAB* gene and remove the existing Cm^R cassette (present in either the *cyoA* or *appCB* gene locus). Once removed, a Cm^R cassette with homologous regions to the remaining oxidase gene outside cytochrome *bd*-I could be inserted to create a chloramphenicol resistant strain capable of solely expressing the cytochrome *bd*-I oxidase.

The parent strain for engineering a strain with only cytochrome *bd*-I active was MS506, a *cyoA::Cm*^{R} strain lacking cytochrome *bo*'. The Cm^R cassette was excised via Flp-FRT recombination (Section 3.1.1.2). Three colonies that were sensitive to chloramphenicol, yet resistant to gentamicin and ampicillin were selected for screening via colony PCR to confirm Cm^R cassette deletion (Figure 3.3).

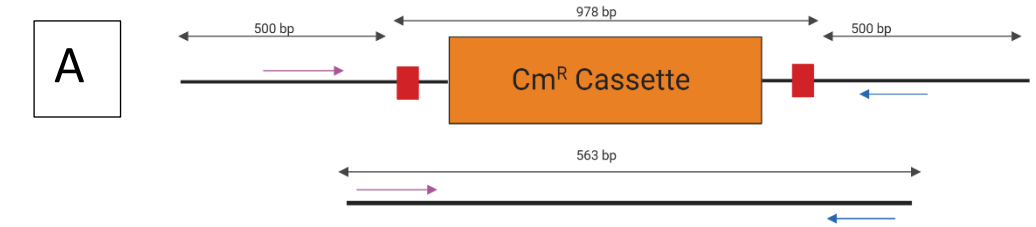

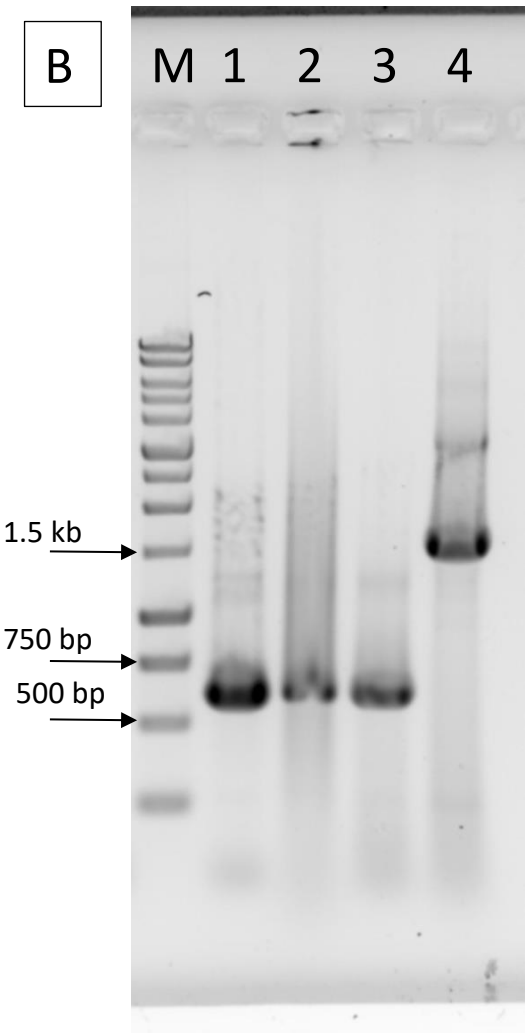

Figure 3.4 Colony PCR to screen for removal of Cm cassette from a cyo::Cm^R strain. A) *Diagram illustrating the Cm^R cassette present in cyoA mutant MS506 with 500 bp regions of homology on each side of the gene locus. The screening primers (#271 and #272) used to confirm excision of Cm^R cassette produced a 1541 bp fragment when the cassette is present or 563 bp when the cassette has been removed.* ***B)*** *1 % agarose gel showing colony PCR products. Lane M) Promega 1 kb DNA ladder. Lanes 1-3) Three Cm^S colonies obtained following an FRT flippase reaction were screened to test if the Cm^R cassette had been successfully removed. Lane 4) A cyoA::Cm^R colony (MS506) was screened with cyoA primers as a positive control.*

A PCR product of 563 bp was observed, corresponding to the correct size of fragment for a *cyoA* strain without the Cm^R cassette (Figure 3.3B).

The *cyoA::*Cm^S strain, MS623, was then inserted with pKOBEG_Gm (encodes λ-Red machinery), and was used to replace the *appCB* gene with a Cm^R cassette with the appropriate homologous regions (Section 3.1.1.3). Colonies growing on LB Cm agar following the λ-Red experiment were screened to ensure no contamination occurred. Desired colonies were resistant to gentamicin (pKOBEG_Gm plasmid), chloramphenicol (Cm^R cassette), and ampicillin (EC958 strains are intrinsically resistant to ampicillin). Colonies that met these criteria

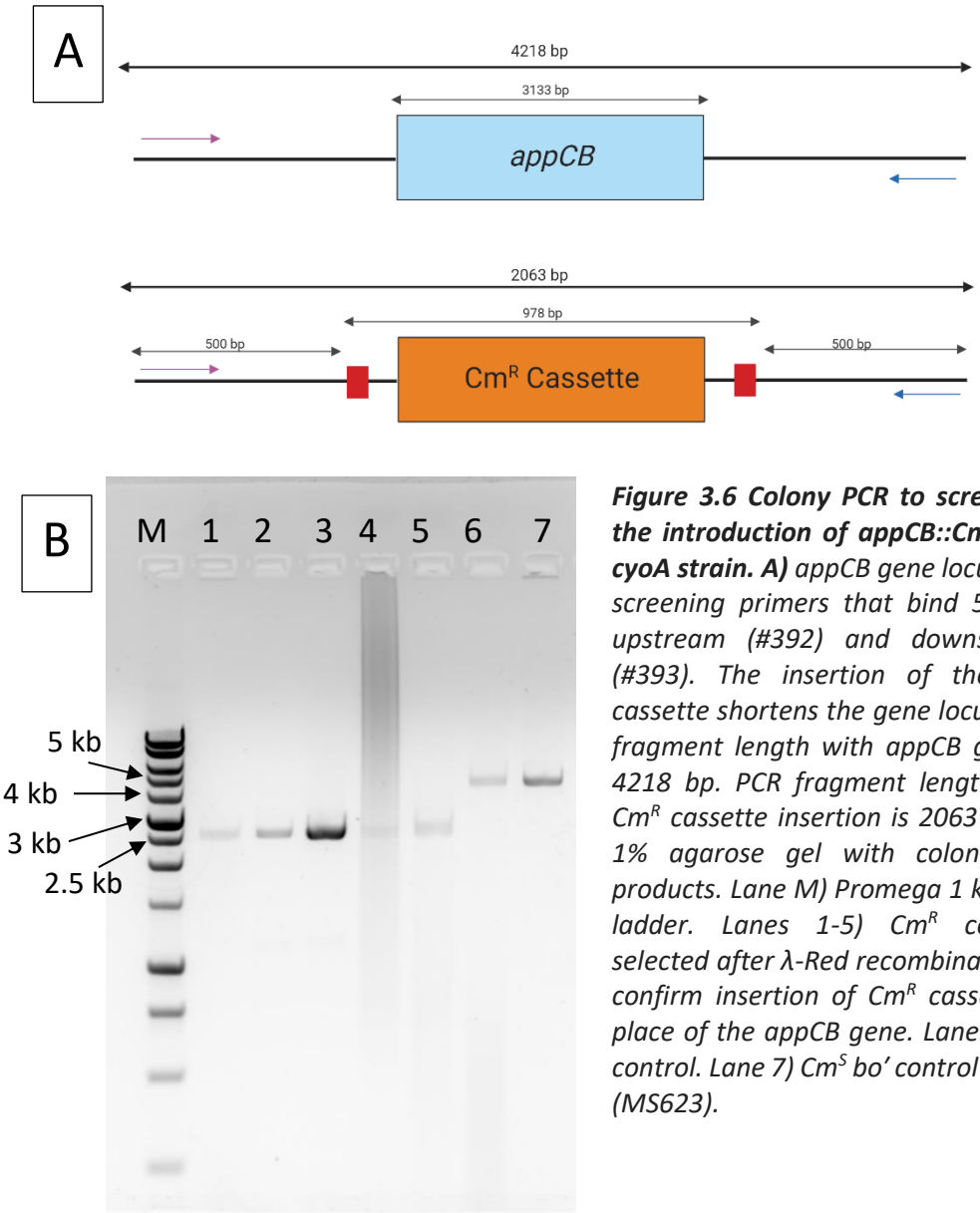

Figure 3.6 Colony PCR to screen for the introduction of appCB::*Cm^R *in a cyoA strain. A) *appCB gene locus with screening primers that bind 500 bp upstream (#392) and downstream (#393). The insertion of the* Cm^R *cassette shortens the gene locus. PCR fragment length with appCB gene is 4218 bp. PCR fragment length with* Cm^R *cassette insertion is 2063 bp.* ***B)*** *1% agarose gel with colony PCR products. Lane M) Promega 1 kb DNA ladder. Lanes 1-5)* Cm^R *colonies selected after λ-Red recombination to confirm insertion of* Cm^R *cassette in place of the appCB gene. Lane 6) WT control. Lane 7)* Cm^S *bo' control colony (MS623).*

were screened via colony PCR to confirm insertion of the Cm^R cassette at the *appCB* locus (Figure 3.4): PCR products of roughly 2500 bp were observed, and subsequently sequenced to confirm *appCB* deletion (data not shown).

3.1.3. Engineering a 'cytochrome *bd*-II only' strain

The strategy in achieving a mutant only able to express cytochrome *bd*-II, *appCB* expression, was to begin with a single KO mutant still containing the *appCB* gene and remove the existing Cm^R cassette (present in either the *cyoA* or *cydAB* gene locus). Once removed, a Cm^R cassette with homologous regions to the remaining oxidase gene outside cytochrome *bd*-II could be inserted to create a chloramphenicol resistant strain capable of solely expressing the cytochrome *bd*-II oxidase. The parent strain for this mutant was MS16, a *cydAB::*Cm^R strain deficient in cytochrome *bd*-I. The chloramphenicol cassette was flipped out via Flp-FRT recombination by Calum Webster in the Shepherd laboratory creating strain MS614.

A *cydAB::*Cm^S strain, MS614, was utilized to perform the λ-Red recombination experiment as described in Section 3.1.1.3. Colonies exhibiting resistance to chloramphenicol, gentamicin, and ampicillin were screened via colony PCR to confirm Cm^R cassette insertion at the *cyoA* locus (Figure 3.5). The *cyoA* locus (948 bp) is nearly the same size as the Cm^R cassette (978 bp) (Figure 3.5A); therefore, a primer that bound to the Cm^R cassette (#422) was paired with a *cyoA* reverse primer (#426). The expected PCR product of 678 bp was observed (Fig 3.5B). Confirmation via sequencing had not been successful at the time this thesis was submitted.

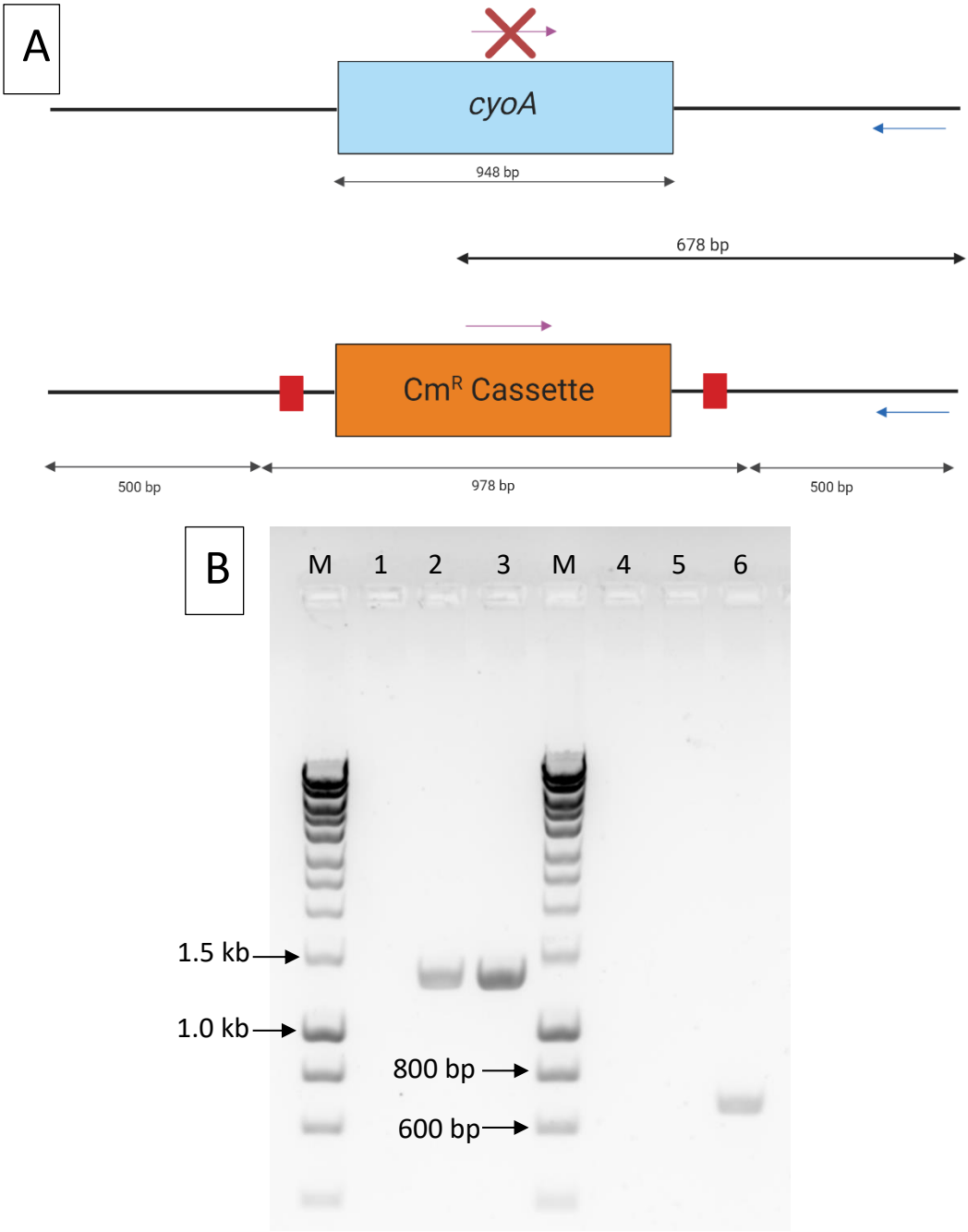

Figure 3.5 Colony PCR to confirm the introduction of cyoA::Cm^R in a cydAB strain. A) *Diagram illustrating sizes of colony PCR fragments when the Cm^R primer (#422) and cyoA reverse primer (#426) are introduced to the cyoA locus. When the cyoA gene was present, no binding occurred. When the Cm^R cassette was present, a 678 bp fragment occurred.* ***B)*** *1% agarose gel depicting colony PCR products confirming a ΔcydAB cyoA::Cm^R genotype. Lanes M) Bioline Hyperladder™ 1kb ladder. Lane 1) Control WT (MS10) strain with cydAB screening primers (#394/#417); expected length: 3868 bp. Lane 2) Control cydAB strain (MS625) with cydAB screening primers; expected length: 1144 bp. Lane 3) cydAB cyoA::Cm^R strain (MS630) with cydAB screening primers; same expected length as MS625. Lane 4) Control WT strain with Cm^R confirmation primers (#422/#426). No fragment expected. Lane 5) cydAB strain with Cm^R confirmation primers. No fragment expected. Lane 6) cydAB cyoA::Cm^R strain with Cm^R confirmation primers: 678 bp fragment expected.*

3.2. Investigating the Relationship between NO-Mediated Respiratory Inhibition and Gentamicin Susceptibility

Previous studies have linked antibiotic efficacy to respiration (Lobritz, et al., 2015). Hence, to explore the relationship between NO, antibiotic lethality, and respiration, respiratory knockouts (KO) were used. Strains only able to express one respiratory oxidase were used to determine the contribution of each terminal oxidase to respiration and protection against gentamicin in the presence of NO. Strains used in the following experiments consisted of a wild type *E. coli* ST131 EC958 strain (**bo' bdI bdII**, MS10), a cytochrome *bd*-I active strain (bo' **bdI** bdII, MS628), a cytochrome *bo*' active strain (**bo'** bdI bdII, MS629), and a cytochrome *bd*-II active strain **(**bo' bdI **bdII**, MS630).

3.2.1. NO and gentamicin antagonistically effect terminal oxidase activity resulting in decreased antibiotic susceptibility

In order to address hypothesis 1 (i.e. NO will diminish the efficacy of the aminoglycoside gentamicin), viability assays to measure the gentamicin-mediated killing of WT *E. coli* EC958 were conducted in the presence and absence of NO-releasing compound GSNO (Section 2.1.7.2). An early exponential phase (OD_{600} 0.3) culture grown in M9 media was exposed to 15 mM of GSNO for 30 min. After pre-exposure to NO, the culture was treated with various concentrations of gentamicin for 90 min. Colony forming units (CFUs) were used to calculate percent survival (Figure 3.6) then plotted and used to calculate the IC_{90} of gentamicin in the presence and absence of NO (Figure 3.7A). The assay featured two controls without exposure to gentamicin; the CFU/mL counts were averaged and used for data normalization as a '100 % survival' control. IC_{90} was calculated for each of the three technical repeats of each biological repeat. At least two independent biological repeats were conducted for each strain. The data clearly demonstrate a large increase in IC_{90} in the presence of GSNO (19.96 µg/mL in the absence of GNSO and 146.0 µg/mL in the presence of GSNO, *P*=.0213; Figure 3.7A & E), which

is consistent with NO diminishing the efficacy of gentamicin killing and the acceptance of hypothesis 1.

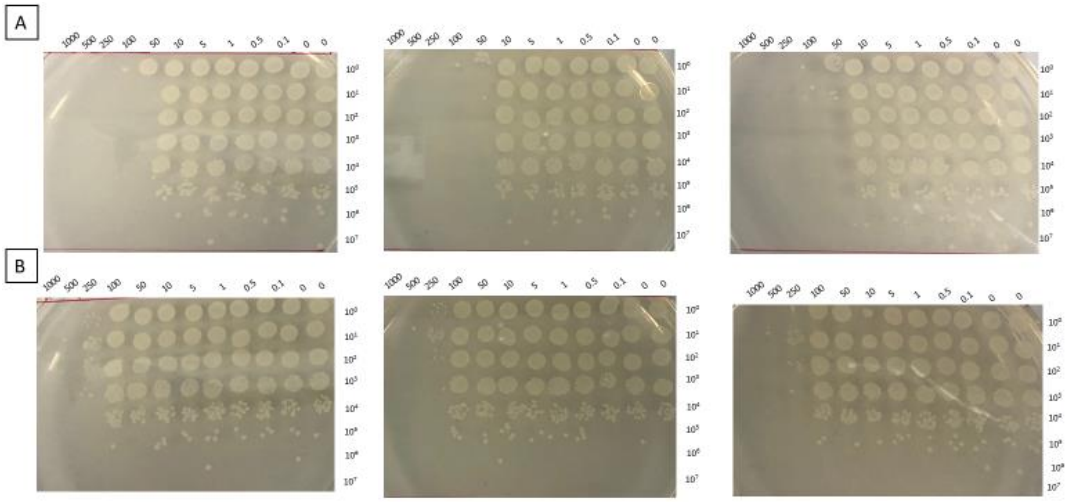

Figure 3.6 Nitric Oxide protects E. coli from the lethal effects of gentamicin. *3 technical repeats of the survival assay of a WT E. coli ST131 EC958 strain in the absence (**A**) or presence (**B**) of GSNO.*

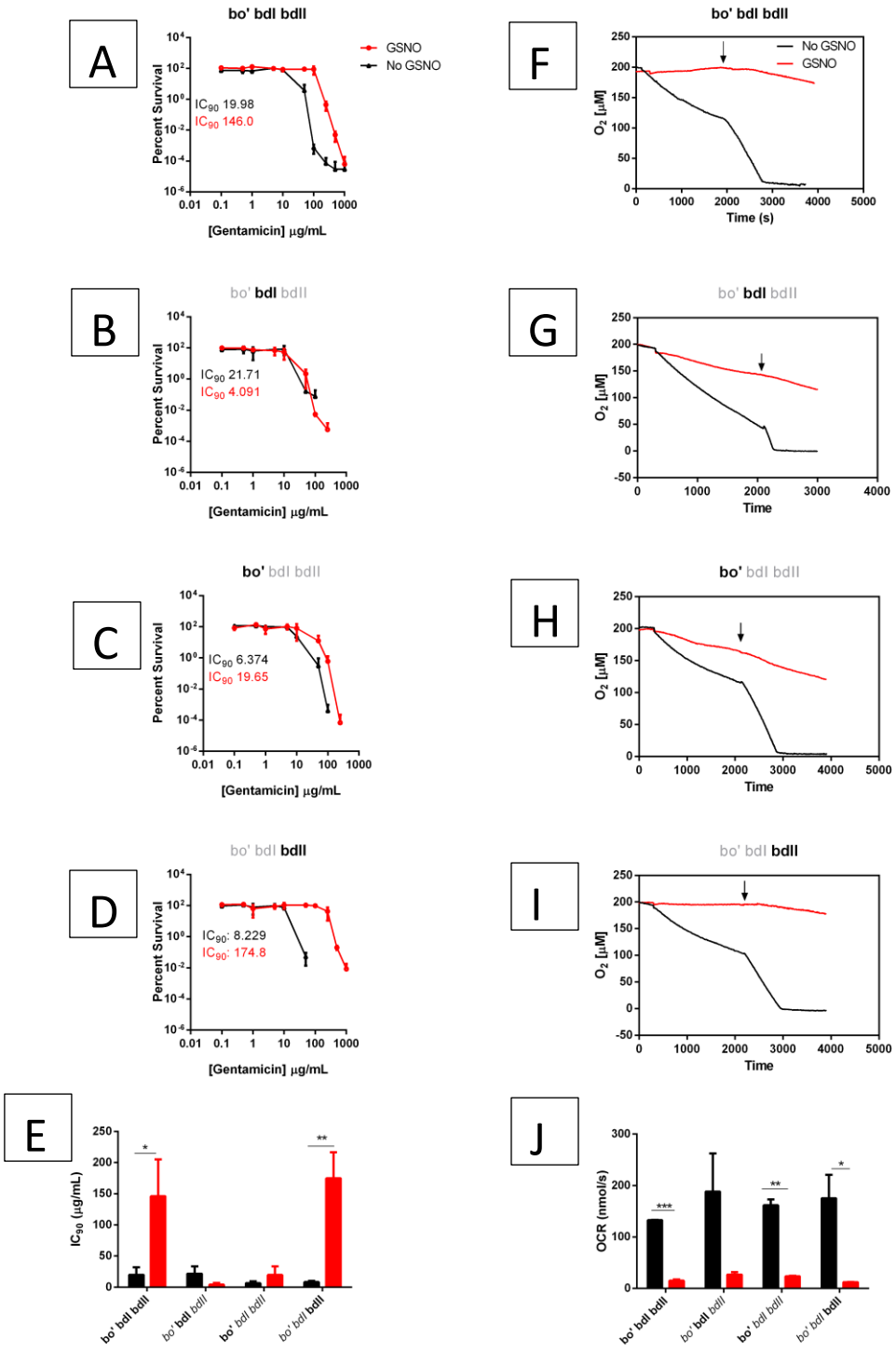

Figure 3.7 Decrease in gentamicin lethality in the presence of NO is linked to aerobic respiration. A-D) *Cell survival of strains plotted against various concentrations of gentamicin. Data points reflect the mean and SD of at least three replicated from two independent assays.* ***E)*** *IC_{90} of gentamicin in the presence or absence of GSNO.* ***F-I)*** *Oxygen consumption traces in the presence or absence of NO. Black arrow denotes gentamicin addition and plunger placement.* ***J)*** *Oxygen consumption rates (OCR) of strains in the presence and absence of NO. (Student's unpaired t-test *: $p < 0.05$, **: $p < 0.005$).*

To test hypothesis 2 (i.e. the *bd*-type oxidases will promote antibiotic-mediated killing in the presence of NO), similar viability assays were undertaken for *bd*-I only, *bo'* only, and *bd*-II only strains (Figure 3.7B-D). These data demonstrate the terminal oxidases do not act similarly when exposed to NO. The presence of only the *bd*-I oxidase showed a trend to promote killing in the presence of NO (average GSNO exposed IC_{90} is 4.091 µg/mL while average untreated IC_{90} is 21.71 µg/mL); however, the data is not statistically significant. The *bo'* and *bd*-II only strains showed resistance to killing in the presence of NO, yet the *bd*-II strain had the only significant change seen ($P< .005$). Cumulatively these data do not support hypothesis 2; although the *bd*-I only strain shows a trend for promoting antibiotic-mediated killing in the presence of NO the data is not statically sound and more robust experimentation needs to be done.

It was anticipated that a decrease in gentamicin killing would coincide with a decrease in aerobic respiration. To confirm this, oxygen consumption measurements were gathered under similar conditions as the viability assays (Section 2.1.8). The oxygen traces for wild type and the double knockout mutant strains are presented in Figure 3.7F-I. These data clearly demonstrate respiratory

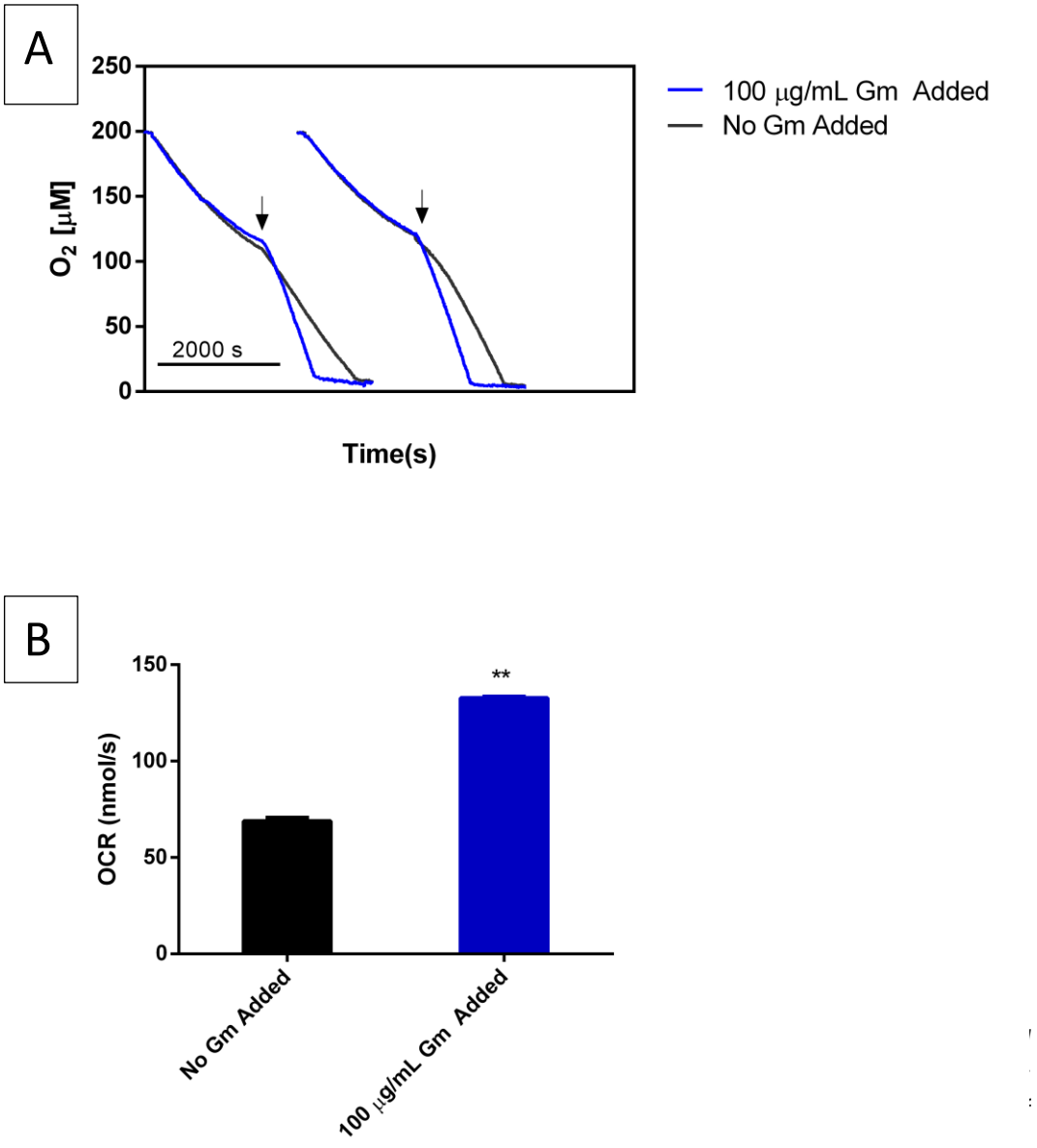

Figure 3.8 Gentamicin elevates aerobic respiration in pathogenic E. coli. A) *2 biological repeats of WT E. coli oxygen consumption traces. Black arrow denotes when plunger is placed on chamber.* ***B)*** *Oxygen consumption rates of E. coli in the presence or absence of gentamicin. (Students unpaired t-test; **: $p < 0.005$)*

inhibition in the presence of NO. This is antagonistic to the ability of gentamicin to increase respiratory rates in *E. coli* (hypothesis 3; Figure 3.8). The oxygen consumption rates (OCR) are shown in Figure 3.7J; the strain expressing cytochrome *bd*-I only was the sole strain to not see significant oxygen consumption loss when exposed to GSNO (*P*= .1982). This observation was hypothesized to contribute to the susceptibility of the *bd*-I only strain to gentamicin when exposed to GSNO. The antagonistic effects to respiratory activity of the bactericidal gentamicin and GSNO was thought to protect the WT strain via inhibition of a universal ROS-mediated mechanism of bactericidal antibiotics to kill bacteria. Since respiratory activity in the GSNO-exposed *bd*-I only strain was determined to be statistically similar to the absence of GSNO, similar levels of aerobic respiratory-derived ROS were hypothesized to exist.

3.2.2. Both gentamicin and NO increase ROS production

To address hypothesis 4 (i.e. gentamicin will elevate ROS production in *E. coli*, whilst NO will counteract this), it was imperative to measure ROS production in *E. coli* after exposure to gentamicin, both with and without pre-exposure to GSNO. The ROS assay was designed to mirror the survival assays and oxygen consumption experiments as closely as possible; hence, ROS production was measured in the wild type strain to observe the impact NO exposure on ROS production (Section 2.1.9). ROS production in the double mutant strains was not collected due to time constraints. Bacterial cultures were grown in M9 minimal media until early-log phase was reached. Cells were diluted with or without GSNO and dyed with a ROS Assay Stain available from the Thermo Fisher Scientific Total Reactive Oxygen Species (ROS) Assay Kit 520 nm. After 30 minutes incubation at 37°C, two technical repeats from each biological repeat (two total) were gathered. Gentamicin was added at the appropriate concentration and cultures were incubated for 30 or 90

additional minutes. Once samples were collected, they were stained with DAPI and fixed as described in Section 2.1.9.2.

The data reveal a large increase in ROS production in comparison to the basal rate 30 minutes post gentamicin treatment which is then decreased after 90 minutes of gentamicin exposure (Figure 3.9). Pre-exposure to GSNO did not elicit a change in ROS production after 30 minutes of gentamicin exposure; however, 90 minutes post gentamicin treatment, GSNO significantly (*P*=.0430) increased ROS production in *E. coli* (Figure 3.9). This finding supports the claim that gentamicin increases ROS production in *E. coli*, but contrary to initial thought, NO enhances this observation.

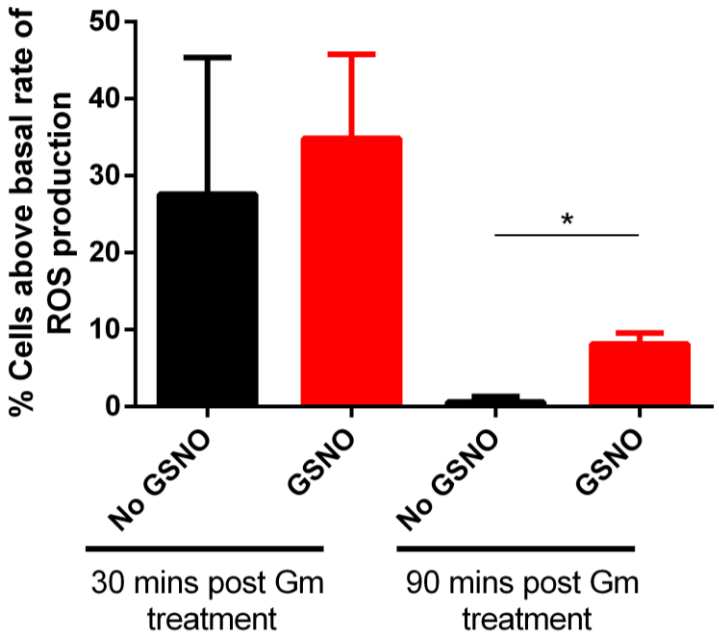

Figure 3.9 ROS production at various time points in the presence and absence of NO. *WT E.coli experiences significant increase in ROS production after 30 minute exposure to gentamicin and after 90 minutes exposure to gentamicin total ROS is reduced. Pre-exposure to GSNO elevates ROS production at 90 minutes. (Student's unpaired t-test; *: p < 0.05).*

Chapter 4

Discussion

4.1. Engineering Sole Oxidase Mutants

4.1.1. Introduction

Mutants lacking a single oxidase can be helpful when determining the contribution to aerobic respiration, or lack thereof when exposed to antibiotic and NO. However, it has been demonstrated that in a cytochrome *bd*-I KO strain, cytochrome *bd*-II among other genes may compensate for the lost function of cytochrome *bd*-I (Shephed, et al., 2010). Therefore, in order to address the proposed hypotheses (Section 1.4), respiratory mutants expressing a sole known oxidase were necessary to assess the contributions of each terminal oxidase to protection during infection (i.e. in the presence of NO) from antibiotics without interference from an additional oxidase.

To achieve mutants possessing only one out of the three terminal oxidases present in *E. coli*, a simple method was adapted from Datsenko and Wanner (2000). Lambda-Red recombination and Flp-FRT recombination were used to excise the desired oxidase gene from the chromosomal genome. After several initial attempts failed to produce results, success was achieved when changes were made to the media used to make the electrocompetent cells for the λ-Red experiment (Section 3.1.1.).

4.1.2. An optimized protocol for λ-red recombination

The original protocol adapted from Datsenko and Wanner (2000) initially failed to produce results. Cells carrying a helper plasmid with λ-red proteins were grown in SOB supplemented with gentamicin and 20 mM of L-arabinose to induce the λ-red proteins. This culture was grown at 28°C until an OD_{600} of 0.4-0.8 was reached. Cells were made electrocompetent by concentrating 250-fold and washing three times in ice-cold 10% (v/v) glycerol. 40 µL (8×10^7 cells/µL) of λ-Red expressing electrocompetent cells were added to a chilled cuvette then 16 µL (approximately 70 ng/mL) of purified DNA was mixed in. After electroporation, cells were recovered in 1 mL of SOC for 1 hour at 37°C. 100 µL of cells were added

to a selective plate and incubated overnight. If no colonies grew, the remaining culture would be plated following static incubation at room temperature.

Methodical and systematic changes were introduced into the aforementioned method until successful mutants were achieved. A longer recovery time in pre-warmed SOC, gentle centrifugation steps during electrocompetent cell procedure, and harvesting cells earlier in log-phase were steps taken to address the failed λ-red experiments. The strains used for the experiment already lacked one terminal oxidase (essential for effective aerobic respiration), thus it was hypothesized knocking out an additional oxidase would cause significant growth impediment to the transformed strain. Subsequently, selection plates with recovered culture were left to incubate for up to 5 days to allow any slow growing colonies to appear, to no avail. The λ-red proteins on the pKOBEG_Gm plasmid (Figure 2.1B) are under control of the P_{BAD} promoter and its regulatory gene *araC*. This common inducible promoter is tightly regulated and will only activate in the presence of L-arabinose and complete absence of glucose (Lee, et al., 1987)**.** Further investigation of this promoter revealed maximum induction when induced in minimal media (Guzman, et al., 1995)**.** When cells containing pKOBEG_Gm were grown in M9 minimal media (excluding the addition of glucose) rather than SOB media and the aforesaid steps were taken, successful results were achieved.

4.2. NO-Mediated Antibiotic Resistance is Linked to Aerobic Respiration

4.2.1. Introduction

Nitric oxide has been of interest to use in novel therapeutics due to its cytotoxicity to bacterial cells and low interaction with mammalian cells (Bogdan, 2001). However, bacteria possess sophisticated systems to evade the cytotoxic effects of NO, including the NO-tolerant terminal oxidase cytochrome *bd*-I. Cytochrome *bd*-I has been implicated to play a vital role in host colonization and is an important defence mechanism during immune attack (Shepherd, et al.,

2016). This finding suggests aerobic respiration contributes significantly to the strategy *E. coli* utilizes in colonizing host cells since cytochrome *bd*-I allows the bacterium to continue to respire under nitrosative stress induced via the immune response. Aerobic respiration has also been linked to a common mechanism of killing by antibiotics through the production of excess reactive oxygen species (Kohanski, et al., 2007). These findings lead to the 4 hypotheses investigated herein:

1. NO will diminish gentamicin efficacy in *E. coli*
2. Cytochrome *bd*-type oxidases will promote gentamicin-mediated killing in the presence of NO
3. Gentamicin will elevate aerobic respiration, while NO will inhibit respiratory function
4. Gentamicin will elevate reactive oxygen species while NO will counteract production of ROS

To investigate each hypothesis, three main experiments were conducted. To determine if NO would decrease gentamicin susceptibility in a pathogenic strain of *E. coli*, viability assays were conducted with NO-exposed cells at varying concentrations of gentamicin as described in Section 2.1.7.2. Similar assays were undertaken in newly engineered single oxidase strains (Section 3.1) to determine if the cytochrome *bd*-type oxidases increase gentamicin susceptibility when pre-exposed to NO. To confirm proposed theories linking bactericidal antibiotics, such as gentamicin, to increased aerobic respiration, oxygen consumption was recorded in the presence and absence of NO after cells were treated with gentamicin (Section 3.2.1.). After correlation of respiratory function and gentamicin-mediated killing was established, investigation of the contribution of ROS production was conducted. To determine if gentamicin elevates ROS production, and if NO directly counteracts this, ROS measurements were collected in WT EC958 *E. coli* (Section 3.2.2.).

4.2.2. Gentamicin and NO antagonistically affect aerobic respiration

A common mechanism in which bactericidal antibiotics (e.g. aminoglycosides) effectively kill bacteria has been proposed as an alternative to the primary mode of action the antibiotics use (Kohanski, et al., 2010). Evidence of altered metabolism (Belenky, et al., 2015) and increased respiration (Lobritz, et al., 2015) in response to bactericidal antibiotics lead to the theory investigated here within. Nitric oxide is an important biomolecule involved in the immune response and targets the terminal oxidases in the respiratory chain of *E. coli* (Borisov, et al., 2004) and has been shown to decrease antibiotic susceptibly in bacteria (Gusarov, et al., 2009). Understanding how the antagonistic effects of antibiotics and a major product of the immune system (e.g. NO) allow bacteria to escape the lethality of antibiotics is crucial in tackling AMR.

It was determined gentamicin significantly increased oxygen consumption when added to a pathogenic strain of *E. coli* (Figure 3.8) while GSNO was confirmed to effectively shut down respiratory function (Figure 3.7F). The ability of GSNO to reduce respiratory function resulted in the increase in survival among cells when exposed to gentamicin (Figure 3.7A &E). Similar experiments were conducted on respiratory mutants to support the correlation between respiratory function and antibiotic susceptibility. No mutants show a difference in killing in the absence of GSNO; however, the wild type and *bd*-II only mutant show a significant difference in survival when exposed to GSNO (Figure 3.7).

4.2.2.1. Lack of respiratory function is linked to decreased susceptibility to gentamicin

Cytochrome *bd*-I has been shown to confer NO-resistance to *E. coli* (Mason, et al., 2009) thusly allowing the bacterium to continue to respire in nitrosative conditions. It was hypothesized the *bd*-type oxidases would promote gentamicin killing when pre-exposed to GSNO since the *bd*-type oxidases are deemed NO-tolerant due to their high dissociation rates with the inhibitory ligand (Borisov, et al., 2011). NO was found to have a profound effect on a wild type strain effectively shutting down respiration and decreasing gentamicin susceptibility (Figure 3.7A &

F). The strain expressing cytochrome *bo'* only was expected to mimic the WT phenotype when treated with gentamicin after pre-exposure to GSNO since *bo'* is the most abundant oxidase in aerobic conditions with seemingly minimal interaction with the low oxygen *bd*-type oxidases. However, the lack of the *bd*-type oxidases clearly made a difference in gentamicin susceptibility in the presence of GSNO as the IC_{90} in the presence of GSNO was significantly (Student's unpaired t-test, $P < .05$) lower than in WT. This difference cannot be explained through respiratory activity investigated within this work.

The NO-tolerant mutant, *bd*-I only, experienced no significant difference in killing in the presence of GSNO compared to the absence of GSNO after treatment with gentamicin (Figure 3.7B &E). This strain also displayed no significant decrease in oxygen consumption when exposed to GSNO (Figure 3.7J). Though these combined findings support the NO-tolerant phenotype; they do not support the proposed hypotheses that sustained respiratory function results in increased gentamicin susceptibility. However, more robust investigation of the newly engineered mutants should be undertaken to confirm findings within.

Cytochrome *bd*-II, although a *bd*-type oxidase, was shown to be severely inhibited by GSNO (Figure 3.7I) and consequently exhibited the highest amount of protection from GSNO against gentamicin-mediated killing (Figure 3.7D & E). These findings support the proposed hypotheses that inhibition of respiratory activity limits the susceptibility to gentamicin-mediated killing.

The phenotypes exhibited by WT and the mutant *bd*-II only strain support the claim that aerobic respiration is intimately involved in antibiotic efficacy Respiration data (Figure 3.7F-J) also support the theory increased metabolic activity leading to increased ROS may be involved in the pathway of killing by gentamicin. Since GSNO and gentamicin act opposite to each other in regards to aerobic respiration, it was hypothesized ROS production would be increased by gentamicin but significantly reduced by NO thusly explaining the protection provided by GSNO.

4.2.2.2. ROS production is influenced by gentamicin and NO

A by-product of aerobic respiration is the creation of common reactive oxygen species such as superoxide and hydrogen peroxide (Imlay, 2003); ROS are also theorized to be a major contributor to antibiotic-mediated killing (Kohanski, et al., 2010) (Figure 1.5). Gentamicin was determined to increase respiration (Figure 3.8), thus it was hypothesized an increase in ROS would be observed and GSNO would counteract this production (Figure 1.8). ROS production was seen to significantly increase at 30 minutes post gentamicin treatment with a sharp reduction at 90 minutes post gentamicin treatment (Figure 3.9). This suggests a major oxidative burst occurs shortly after the introduction of gentamicin. Since NO was shown to inhibit aerobic respiration (Figure 3.7), it was surprising to discover GSNO promoted ROS production rather than reduced ROS as proposed (Figure 3.9). This finding has prompted an alternative explanation for the results described above.

NO effectively shuts down aerobic respiration by binding to the NO-sensitive terminal oxidases in *E. coli,* consequently inhibiting oxidase function. Aminoglycosides, along with other classes of bactericidal antibiotics, have been shown to hyperactivate the TCA cycle leading to excess NADH availability and upregulation of NADH dehydrogenase I (Ndh-I) (Kohanski, et al., 2007). As Ndh-I effectively catalyses the protonation of ubiquinone (Q) to ubiquinol (QH_2), QH_2 accumulates within the membrane to be oxidized. With the terminal oxidases shut down by NO, QH_2 is unable to be oxidized thus beings to build-up within the membrane. Some trigger (perhaps pressure to return to homeostatic conditions) influences QH_2 to donate electrons to dioxygen within the cytosol creating

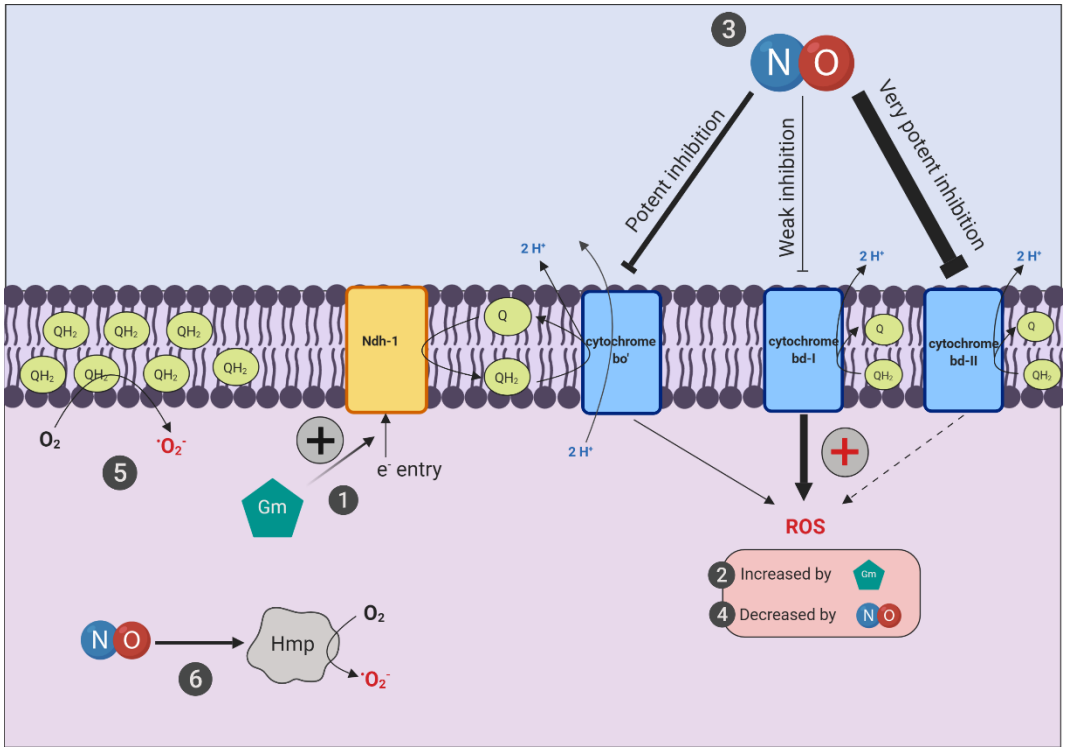

Figure 4.1 Model for the impact of NO upon ROS generation in E. coli. 1) *Gentamicin stimulates hyperactivation of the TCA cycle promoting e^- donors to enter the ETC and increase respiration.* ***2)*** *Gentamicin stimulates excess ROS production via increased respiration.* ***3)*** *NO differentially inhibits the terminal oxidases and decreases respiration.* ***4)*** *NO-mediated respiration inhibition diminishes ROS generation.* ***5)*** *Build-up of ubiquinol (QH_2) due to NO-mediated respiratory inhibition increases ROS.* ***6)*** *Overexpression of Hmp in response of NO increases ROS production.*

superoxide (O^-_2) ions (Figure 4.1[5]). The NO-detoxifying enzyme Hmp is also upregulated in periods of nitrosative stress (Gardner, et al., 1998) (Poole, et al., 1996). A by-product of Hmp's ability to detoxify the cell of NO, is the production of superoxide that also contributes to oxidative stress (Membrillo-Hernandez, et al., 1996) (Figure 4.1[6]). Evidence of a NO-induced oxidative response has also been demonstrated through upregulation of the *sosRX* regulon offering additional support to the aforementioned results (Nunoshiba *et al.* 1993; Nunoshiba *et al.* 1995).

4.3. Model for Gentamicin Lethality in the Presence of NO in Pathogenic *E. coli*

Building upon work demonstrating NO-tolerant oxidase cytochrome *bd*-I offers protection against antibiotics during infection (Shepherd, et al., 2016), it

was important to investigate the mechanism in which this is facilitated. Herein, it has been shown that NO shuts down respiratory function allowing *E. coli* to escape the lethal consequences of antibiotics. This protection does not come from the reduction of ROS as initially thought since NO promotes the formation of ROS. Eliminating this possibility allows for another theory to come to the focus. The protection NO offers may be due to a depleted proton gradient (Δψ) stemming from lack of terminal oxidase activity. Gentamicin is a highly positively charged molecule (Figure 4.2A); therefore, the Δψ provided by the ETC may be a driving force of gentamicin entry into the cell (Bryan & Kwan, 1983) (Hancock, 1981). Once in the cell, gentamicin can perform the primary mode of action (attach to the 30S ribosomal unit and promote mistranslation of proteins) and kill the bacterium (Figure 4.2B). NO inhibits terminal oxidase activity, which may reduce the Δψ significantly limiting gentamicin entry. Any contribution of ROS resulting from gentamicin induced respiration seems to be inconsequential to antibiotic susceptibility since the condition in which the most ROS is produced is the same condition that effectively avoids gentamicin lethality (Figure 4.2B).

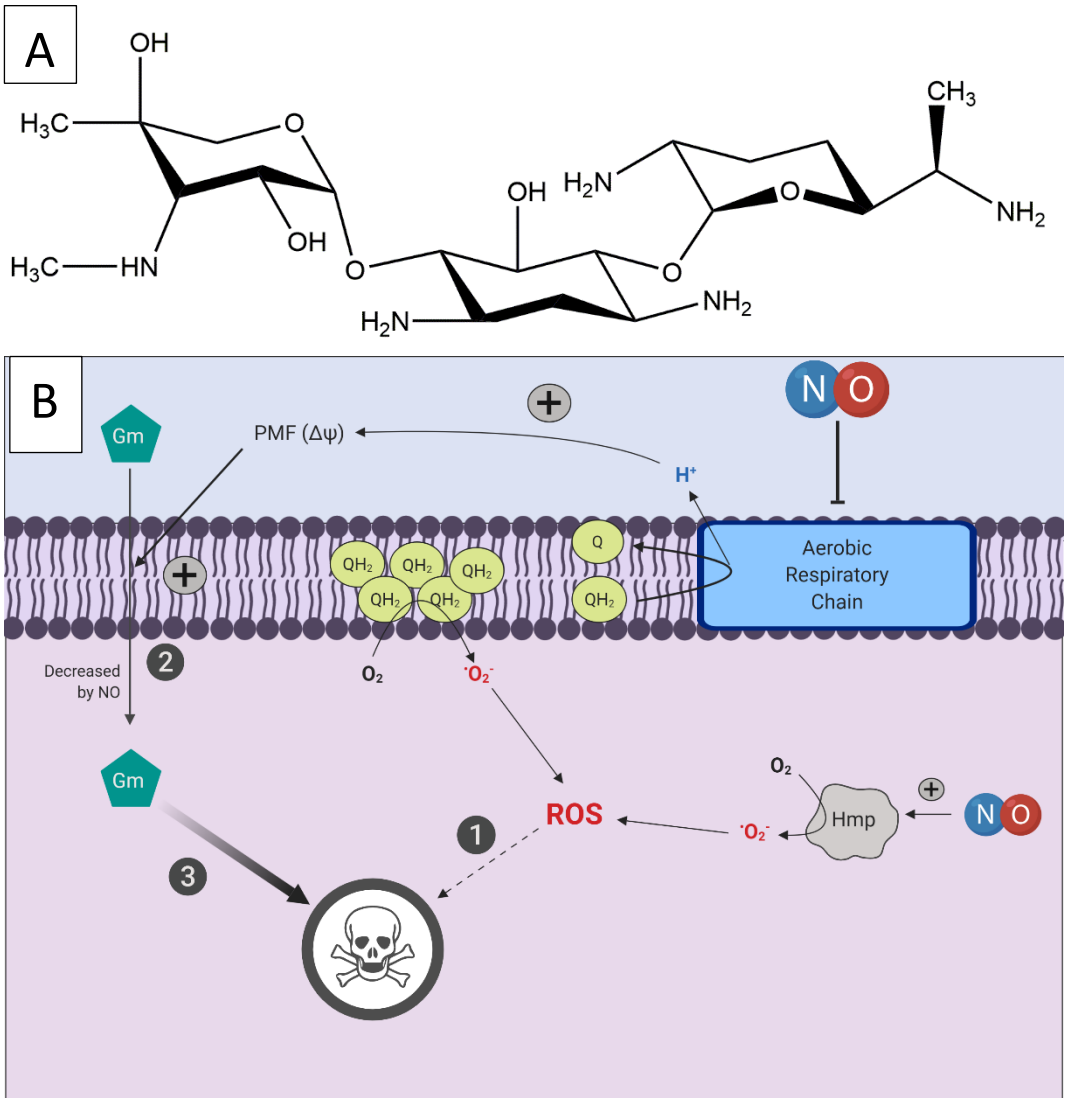

Figure 4.2 Model for gentamicin lethality in the presence of NO. A) *Gentamicin is a highly positively charged molecule. A large pmf (Δψ) may be a driving factor for entry into the cell.* ***B) 1)*** *Increased ROS in the presence of NO has negligible effect on cell death.* ***2)*** *NO-mediated respiratory inhibition decreases Δψ, which diminishes gentamicin entry into the cell.* ***3)*** *The main mechanism of gentamicin-mediated cell death is the primary mode of action for the antibiotic and this is diminished by NO.*

4.4. Future Research

Though this work has solidified the relationship between antibiotics and respiration, much work needs to still be conducted to determine the role the immune system plays in antibiotic susceptibility. GSNO was found to induce ROS production in a wild type strain; hence, future research should be undertaken to determine if this pattern is also seen in strains lacking one or more respiratory

complexes. It was proposed the NO-detoxifying enzyme Hmp contributes significantly to the excess ROS seen when the cell is exposed to GSNO; therefore, measuring ROS production in a *hmp* knockout would be useful in determining if this theory is correct. To investigate the hypothesis put forward implicating the role of the proton gradient (Δψ) in gentamicin entry into the cell, gentamicin uptake assays and sensitive PMF measurements should be carried out in the presence and absence of GSNO.

This work concentrates on the specific mechanisms of gentamicin evasion in pathogenic *E. coli* ST131 EC958 with the use of NO-donor GSNO. While Kohanski and colleagues (2010) detail β-lactams and quinolones as other antibiotic classes alongside aminoglycosides which are involved in a common metabolism-related mechanism for antibiotic induced cell death, it will be helpful to test the theories developed within this body of work, i.e. a common mechanism of antibiotic resistance resulting from NO-mediated Δψ depletion, to antibiotic classes emphasised to utilize this pathway. Alternative NO-donors, such as NOC-12 (NO-releaser with extended half-life) or SNP (sodium nitroprusside) should also be utilized to determine if a common mechanism can truly be detailed in relation to bactericidal antibiotics and NO-mediated inhibition. Furthermore, to fully understand the mechanism *in vivo* and determine novel therapeutics, it is important to consider the effect of macrophage-derived NO on antibiotic susceptibility and how iNOS inhibitors (e.g. L-NAME) alter antibiotic efficacy. Extending that line of work further, it will be interesting to determine infection rate in mice with iNOS -/- phenotype and how antibiotic susceptibility is further altered.

A clear understanding of this mechanism will allow researchers to focus on exploiting this knowledge and develop therapeutics that control immune NO release during aggressive antibiotic courses. The findings herein also should be considered when developing therapeutics that may contain NO-releasing compounds as it may inadvertently promote antibiotic resistance rather than reduce it as planned.

References

Aldred, K., Kerns, R. & Osheroff, N., 2014. Mechanism of quinolone action and resistance. *Biochemistry,* pp. 1565-74.

Almeida, C. et al., 2006. The Role of the Hybrid Cluster Protein in Oxidative Stress Defense. *The Journal of Biological Chemistry,* 281(43), pp. 32445-50.

American Chemical Society International Historic Chemical Landmarks, n.d. *Discovery and Development of Penicillin.* [Online]
[Accessed 12 11 2018].

Aminov, R., 2010. A brief history of the antibiotic era: lessons learned and challenges for the future.. *Frontiers of Microbiology,* 08 12.1(134).

Atlung, T. & Brondsted, L., 1994. Role of the transcriptional activator AppY in regulation of the *cyx appA* operon of *Escherichia coli* by anaerobiosis, phosphate starvation, and growth phase. *Journal of Bacteriology,* 176(17), pp. 5414-5422.

Barlow, M., 2009. What Antimicrobial Resistance Has Taught Us About Horizontal Gene Transfer. In: *Methods in Molecular Biology.* s.l.:Humana Press, pp. 397-411.

Barlow, M., Reik, R., Jacobs, S. & al, e., 2008. High Rate of Mobilization for blaCTX-Ms. *Emerging Infectious Diseases,* 03, 14(3), pp. 423-428.

Bekker, M. et al., 2010. The ArcBA Two-Component System of *Escherichia coli* Is Regulated by the Redox State of both the Ubiquinone and Menaquinone Pool. *Journal of Bacteriology,* pp. 746-754.

Bekker, M. et al., 2009. Respiration of *Escherichia coli* Can Be Fully Uncoupled via the Nonelectrogenic Terminal Cytochrome *bd*-II Oxidase. *JOURNAL OF BACTERIOLOGY,* 191(17), pp. 5510-5517.

Belenky, P. et al., 2015. Bactericidal Antibiotics Induce Toxic Metabolic Perturbations that Lead to Cellular Damage. *Cell Reports,* 13(5), pp. 968-80.

Bogdan, C., 2001. Nitric oxide and the immune response. *Nature Immunology,* 2(10), pp. 907-917.

Bonamore, A. & Boffi, A., 2007. Flavohemoglobin: Structure and reactivity. *IUBMB Life ,* December, 60(1), pp. 19-28.

Bonamore, A. et al., 2003. *Escherichia coli* Flavohemoglobin Is an Efficient Alkylhydroperoxide Reductase. *The Journal of Biological Chemistry,* 278(25), pp. 22272-22277.

Borisov, V. et al., 2008. Glutamate 107 in Subunit I of Cytochrome *bd* from *Escherichia coli* Is Part of a Transmembrane Intraprotein Pathway Conducting Protons from the Cytoplasm to the Heme b595/Heme d Active Site. *Biochemistry,* pp. 7907-7914.

Borisov, V. et al., 2004. Interaction of the bacterial terminal oxidase cytochrome *bd* with nitric oxide. *FEBS Letters,* pp. 201-204.

Borisov, V., Gennis, R., Hemp, J. & al., e., 2011. The cytochrome *bd* respiratory oxygen reductases. *NIH Public Access,* 1807(11), pp. 1398-1413.

Boucher, H., Talbot, G., Benjamin, D. & al., e., 2013. 10 x 20' Progress--Development of New Drugs Active Aganist Gram-Negative Bacilli: An Update From the Infectious Diseases Society of America. *Clinical Infectious Diseases,* 15 06, 56(12), pp. 1685-1694.

Bryan, L. & Kwan, S., 1983. Roles of ribosomal binding, membrane potential, and electron transport in bacterial uptake of streptomycin and gentamicin. *Antimicrobial Agents and Chemotherapy,* 23(6), pp. 835-845.

Center for Disease Contol and Prevention, 2013. *Antibiotic Resistance Threats in the United States, 2013,* s.l.: s.n.

Centers for Disease Control and Prevention, 2018. *Biggest Threats and Data.* [Online]
[Accessed 09 10 2018].

Corker, H. & Poole, R., 2003. Nitric Oxide Formation by *Escherichia coli* dependence on nitirite reductase, the NO-sensing regulator Fnr, and flavohemoglobin Hmp. *Journal of Biological Chemistry,* August, 278(34), pp. 31584-92.

Cotter, P. A., Chepuri, V., B., G. R. & Gunsalus, R. P., 1990. Cytochrome o (cyoABCDE) and d (cydAB) oxidase gene expression in *Escherichia coli* is regulated by oxygen, pH, and the fnr gene product. *Journal of Bacteriology,* 172(11), pp. 6333-6338.

Cotter, P. A., Melville, S. B., Albrecht, J. A. & Gunsalus, R. P., 1997. Aerobic regulation of cytochrome d oxidase (cydAB) operon expression in *Escherichia coli*: roles of Fnr and ArcA in repression and activation. *Molecular Microbiology,* 25(1), pp. 605-615.

Crane, B., 2008. The enzymology of nitric oxide in bacterial pathogensis and resistance. *Biochemical Society Transactions,* December, 36(6), pp. 1149-1154.

Datsenko, K. & Wanner, B., 2000. One-Step inactivation of chromosomal genes in Escherichia coli K-12 using PCR products. *PNAS.*

Dwyer, D. et al., 2014. Antibiotics induce redox-related physiological alterations as part of the lethality. *PNAS.*

Ezraty, B. et al., 2013. Fe-S Cluster Biosynthesis Controls Uptake of Aminoglycoside in a ROS-less Death Pathway. *Science,* pp. 1583-1587.

Fair, R. & Tor, Y., 2014. Antibiotics and bacterial resistance in the 21st century. *Perspectives in medical chemistry,* Volume 6, pp. 25-64.

Falagas, M., Fragoulis, K. & Karydis, I., 2006. A Comparative Study on the Cost of New Antibiotics and Drugs of Other Therapeutic Categories. *PLoS ONE,* 20 12, 1(1), p. e11.

Farha, M., French, S., Stokes, J. & Brown, E., 2018. Bicarbonate Alters Bacterial Susceptibility to Antibiotics by Targeting the Proton Motive Force. *ACS Infectious Diseases,* Volume 4, pp. 382-390.

Feelisch, M., 1998. The use of niric oxide donors in pharamacological studies. *Naunyn-Schmiedeberg's archives of pharmacology,* 358(1), pp. 113-22.

Fernandes, P. & Martens, E., 2017. Antibiotics in late clinical development. *Biochemical Pharmacology,* 01 06, Volume 133, pp. 152-163.

Fernandez, L. & Hancock, H., 2012. Adaptive and mutational resistance: role of porins and efflux pumps in drug resistance. *Clinical Microbiology Reviews,* 10, 25(4), pp. 661-81.

Filenko, N. et al., 2007. The NsrR Regulon of *Escherichia coli* K-12 Includes Genes Encoding the Hybrid Cluster Protein and the Periplasmic, Respiratory Nitrite Reductase. *Journal of Bacteriology,* May, 189(12), pp. 4410-4417.

Flatley, J. et al., 2005. Transcriptional Responses of *Escherichia coli* to S-Nitrosoglutathione under Defined Chemostat Conditions Reveal Major Changes in Methionine Biosynthesis. *The Journal of Biological Chemistry,* 280(11), pp. 10065-72.

Fleming, A., 1950. *Penicilin.* London: Butterworths Medical Publications.

Forde, B. et al., 2014. The Complete Genome Sequence of *Escherica coli* EC958: A high Quality Reference Sequence for the Globally Disseminated Multidrug Resistanct *E. coli* O25b:H4-ST131 Clone. *PLOS ONE.*

Garcia-Horsmant, J. et al., 1994. The Superfamily of Heme-Copper Respiratory Oxidases. *Journal of Bacteriology,* pp. 5587-5600.

Gardner, A. & Gardner, P., 2002. Flavohemoglobin Detoxifies the Nitric Oxide in Aerobic, but Not Anaerobic, *Escherichia coli*. *The Jorunal of Biological Chemistry,* March, 277(10), pp. 8166-8171.

Gardner, A., Helmick, R. & Gardner, P., 2002. Flavorubredoxin, an Inducible Catalyst for Nitric Oxide Reduction and Detoxification in *Escherichia coli*. *The Journal of Biological Chemistry,* March, 277(10), pp. 8172-8177.

Gardner, P., Gardner, A., Martin, L. & Salzman, A., 1998. Nitric Oxide dioxygenase: an enzymi function for flavohemoglobin. *Proceedings of the National Academy of Sciences of the United States of America,* 95(18), pp. 10378-83.

Gaynes, R., 2017. The Discovery if Penicillin-New Insights After More Than 75 Years of Clinical Use. *Emerging Infectious Diseases,* May, 23(5), pp. 849-853.

Giuffre, A. et al., 2014. Cytochrome *bd* oxidase and bacterial tolerance to oxidative and nitrosative stress. *Biochimichia et Biophysica Acta (BBA)-Bioenergetics,* pp. 1178-1187.

Gomes, C. et al., 2002. A novel type of nitric oxide reductase: *Escherichia coli* flavorubredoxin. *Journal of Biological Chemistry,* Volume 277, pp. 25273-76.

Gomes, C., Vicente, J., Wasserfallen, A. & Teixeira, M., 2000. Spectroscoptic Studies and Characterization of a Novel Electron-Transfer Chain from Escherichia coli Involving a Flavorubredoxin and Its Flavoprotein Reductase Partner. *Biochemisty,* Volume 39, pp. 16230-16237.

Green, G., Lorence, R. & Gennis, R., 1986. Specific overproduction and purification of cytochrome b558 component of the cytochrome d complex for *Escherichia coli*. *Biochemistty,* pp. 2309-14.

Gusarov, K., Shatalin, M., Starodubtseva, M. & al., e., 2009. Endogenous Nitric Oxide Protects Bacteria Aganist a Wide Spectrum of Antibiotics. *Science,* 325(5946), pp. 1380-4.

Guzman, L., Belin, D., Carson, M. & Beckwith, J., 1995. Tight Regulation, Modulation, and High-Level Expression by Vectors Containing the Arabinose P BAD Promoter. *Journal of Bacteriology,* 177(14), pp. 4121-4130.

Hancock, R., 1981. Aminoglycoside uptake and mode of action- with special reference to streptomycin and gentamicin. *Journal of Antibacterial Chemotherapy,* 8(1), pp. 249-276.

Hart, T., 1985. Some Observations concerning the S-nitroso and S-phenylsulphonyl dervatives of L-cysteine and glutathione. *Tetrahedron Letters.*

Hausladen, A., Gow, A. & Stamler, J., 1998. Nitrosative Stress: Metabolic pathway involving the flavohemoglobin. *Proceedings of the National Academy of Sciences of the United States of America,* 95(24), pp. 14100-5.

Henkel, S. et al., 2014. Basic Regulatory Principles of *Escherichia coli*'s Electron Transport Chain for Varying Oxygen Conditions. *PLoS ONE,* p. e107640.

Hetrick, E. et al., 2008. Bactericidal effcacy of nitric oxide-releasing silica nanoparticles. *ACS Nano,* 2(2), pp. 235-246.

Hutchings, M., Mandhana, N. & Spiro, S., 2002. The NorR Protein of *Escherichia coli* Activates Expression of the Flavorubredoxin Gene norV in Response to Reactive Nitrogen Species. *Journal of Bacteriology,* 184(16), pp. 4640-43.

Imlay, J., 2003. Pathways of Oxidative Damage. *Annual Review of Microbiology,* 57(1), pp. 395-418.

Ismail, M. et al., 2017. Association of *Escherichia coli* ST131 lineage with risk of urinary tract infection recurrence among young women. *Journal of Global Antibiotic Resistance,* pp. 81-84.

Jurtshuk, P., 1996. Bacterial Metabolism. In: S. Baron, ed. *Medical Microbiology.* 4 ed. Galveston(Tx): Univeristy of Texas Medical Branch.

Karlinsey, J. et al., 2012. The NsrR regulon in nitrosative stress resistance of *Salmonella enterica serovar Typhimurium*. *Molecular Microbiology,* 85(6), pp. 1179-1193.

Keren, I. et al., 2013. Killing by Bacterialcidal Antibiotics Does Not Depend on Reactive Oxygen Species. *Sceince,* pp. 1213-1216.

Kim, S. et al., 1999. Anoxic function for the *Escherichia coli* flavohaemoglobin (Hmp): reversible binding of the nitric oxide and reduction to nitrous oxide. *FEBS Letters,* 445(2-3), pp. 389-394.

Kohanski, M., Dwyer, D. & Collins, J., 2010. How antibiotics kill bacteria: from targets to networks. *Nature Reviews Microbiology,* pp. 423-435.

Kohanski, M. et al., 2007. A Common Mechanism of Cellular Death Induced by Bacterialcidal Antibiotics. *Cell,* pp. 797-810.

Kohanski, M. et al., 2008. Mistranslation of membrane proteins and two-component system activation trigger aminoglycoside-mediated oxidative stress and cell death. *Cell,* pp. 679-690.

Kong, K., Schneper, L. & Mathee, K., 2010. Beta-lactam Antibiotics: From Antibiosis to Resistance and Bacteriology. *APMIS,* 118(1), pp. 1-36.

Kotra, L., Haddad, J. & Mobashery, S., 2000. Aminoglycosides: Perspectives on Mechanisms of Action and Resistance and Strategies to Counter Resistance. *Antimicrobial Agents ans Chemotherapy,* pp. 3249-56.

Lau, S. et al., 2008. UK epidemic *Escherichia coli* strains A-E, with CTX-M-15 B-lactamase, all belong to the international O25:H4-ST131 clone. *Journal of Antimicrobial Chemotherapy,* 62(6), pp. 1241-1244.

Leclercq, R., 2002. Mechanisms of Resistance to Macrolides and Lincosamides: Nature of the Resistance Elements and Their Clinical Implications. *Clinical Infectious Diseases,* pp. 482-492.

Lee, N., Francklyn, C. & Hamiliton, E. P., 1987. Arabinose-induced binding of AraC protein to aral2 activates the *araBAD* operon promoter. *PNAS,* 84(24), pp. 8814-818.

Liu, Y. & Imlay, J., 2013. Cell Death from Antibiotics Without the Involvement fo Reactive Oxygen Species. *Science,* pp. 1210-1213.

Lobritz, M. et al., 2015. Antibiotic efficacy is linked to bacterial cellular respiration. *PNAS,* pp. 8173-8180.

Lu, P. et al., 2015. The cytochrome *bd*-type quinol oxidase is important for survival of Mycobacterium smegmatis under peroxide and antibiotic-induced stress. *Scientific Reports,* pp. 1-10.

MacMicking, J., Xie, Q. & Nathan, C., 1997. Nitric Oxide and Macrophage Function. *Annual Review of Immunology,* 15(1), pp. 323-50.

Martens, E. & Demain, A., 2017. The antibiotic resistance crisis, with a focus of the United States. *Journal of Antibiotics,* 70(5), pp. 520-526.

Mason, M. et al., 2009. Cytochrome *bd* confers nitric oxide resistance to Escherichia coli. *Nature Chemical Biology,* 5(2), pp. 94-96.

Mazzei, T., Mini, E., Novelli, A. & Periti, P., 1993. Chemistry and mode of action of macrolides. *Journal of Antimicrobial Chemotherapy,* pp. 1-9.

McBee, M. et al., 2017. Production of Superoxide in Bacteria Is Stress- and Cell-State-Dependent: A Gating-Optimized Flow Cytometry Method that Minimizes ROS Measurement Artfacts with Fluroscent Dyes. *Frontiers of Microbiology,* Volume 8, p. 459.

Membrillo-Hernandez, J. et al., 1999. The Flavohemoglobin of *Escherichia coli* Confers Resistance to a Nitrosating Agent, a "Nitric Oxide Releaser," and Paraquat and Is Essential for Transcriptional Responses to Oxidative Stress. *The Journal of Biological Chemistry,* 274(2), pp. 748-754.

Membrillo-Hernandez, J., Ioannidis, N. & Poole, R., 1996. The flavohaemoglobin (HMP) of *Escherichia coli* generates superoxide in vitro and causes oxidative stree in vivo. *FEBS Letters,* 382(1).

Meunier, B. et al., 1995. New Inhibitors of the Quinol Oxidation Sites of Bacterial Cytochromes *bo* and *bd*. *Biochemistry,* pp. 1076-1083.

Michael, C., Dominey-Howes, D. & Labbate, M., 2014. The Antimicrobial Resistance Crisis: Causes, Consequences, and Management. *Frontiers in Public Health,* 16 09, Volume 2, p. 224.

Mills, P. et al., 2008. A combination of cytochrome c nitrite reductase (NrfA) and flavorubredoxin (NorV) protects *Salmonella enterica serovar Typhimurium* aganist killing by NO in anoxic enviroments. *Microbology,* April, 154(4), pp. 1218-1228.

Mogi, T. et al., 2006. Probing the ubiquinol-binding site in cytochrome *bd* by site-directed mutagensis.. *Biochemistry,* pp. 7924-30.

Mohr, S., Stamler, J. & Brune, B., 1996. Posttranslational modification of glyceraldehyde-3-phosphate dehydrogenase by S-nitrosylation and subsequent NADH attachment.. *The journal of biological chemistry,* pp. 4209-14.

Mukhopadhyay, P. et al., 2004. Prominent roles of the NorR and Fur regulators in the Escherichia coli transcriptional response to reactive nitrogen species. *PNAS,* 101(3), pp. 745-750.

Munita, J. & Arias, C., 2016. Mechanisms of Antibiotic Resistance. *Microbiology Spectrum,* April.4(2).

Muscara, M. & Wallace, J., 1999. Nitric Oxide. V. therapeutic potential of nitric oxide donors and inhibitors. *The American journal of physiology,* 276(6 Pt 1), pp. G1313-6.

Nablo, B. & Schoenfisch, M., 2003. Antibacterial properties of nitric oxide-releasing sol-gels. *Journal of Biomedical Materials Research,* 67A(4), pp. 1276-1283.

Nakamura, H., Saiki, K., Mogi, T. & Anraku, Y., 1997. Assignment and Functional Roles of the *cyoABCDE* Gene Products Required for the *Escherichia coli bo*-Type Quinol Oxidase. *Journal of Biochemistry,* pp. 415-421.

Nathan, C. & Cars, O., 2014. Antibiotic Resistance- Problems, Progress, and Prospects. *New England Journal of Medicine,* 371(19), pp. 1761-1763.

Newton, G. & Gennis, R., 1991. In vivo assembly of the cytochrome d terminal oxidase complex of *Escherichia coli* from genes encoding the two subunits expressed on seperate plasmids. *Biochimica et Biophysica Acta (BBA)- Gene Structure and Function,* pp. 8-12.

O'Neill, J., 2015. *Rapid Diagnostics: Stopping unnecessary Use of Antibiotics,* London: Review on Antimicrobial Resistance.

Oost, J. B. A. et al., 1994. The heme-copper oxidase family consists of three distinct types of terminal oxidases and is related to nitric oxide reductase. *FEMS Microbiology Letters,* pp. 1-9.

Osborne, J. & Gennis, R., 1999. Sequence analysis of cytochrome *bd* oxidase suggests a revised topology for subunit I. *Biochimica et Biophysica Acta,* pp. 32-50.

Pacher, P., Beckman, J. & Liaudet, L., 2007. Nitric Oxide and Peroxynitrite in Health and Disease. *Physiological reviews,* 87(1), pp. 315-424.

Page, L., Griffiths, L. & Cole, J., 1990. Different physiological roles of two independent pathways for nitrite reduction to ammonia by enteric bacteria. *Archives of microbiology,* 154(4), pp. 349-54.

Partridge, J. et al., 2007. Transition of *Escherichia coli* from Aerobic to Micro-aerobic Condtions Involved Fast and Slow Reacting Regulatory Components. *Journal of Biological Chemistry,* pp. 11230-37.

Pereira, M., Sousa, F., Veríssimo, A. & Teixeira, M., 2008. Looking for the minimum common denominator in haem–copper oxygen reductases: Towards a unified catalytic mechanism. *Biochimica et Biophysica Acta (BBA) - Bioenergetics,* pp. 929-934.

Petty, N. et al., 2014. Global Dissemination of a multidrug resistant *Escherichia coli* clone. *PNAS,* pp. 5694-5699.

Poock, S. et al., 2002. Respiratory Detoxification of Nitric Oxide by the Cytochrome c Nitrite Reductase of *Escherichia coli*. *The Journal of Biological Chemistry,* June, 277(26), pp. 23664-23669.

Poole, R. et al., 1996. Nitric Oxide, Nitrite, and Fnr Regulation of hmp (Flavohemoglobin) Gene Expresseion in *Escherichia* K-12. *Journal of Bacteriology,* 178(18), pp. 5487-5492.

Poole, R. & Hughes, M., 2000. New functions for the ancient globin family: bacterial responses to nitric oxide and nitrosative stress. *Molecular Microbiology,* 36(4), pp. 775-783.

Public Health England, 2015. *Health Matters: antimicrobial resistance.* [Online] Available at: https://www.gov.uk/government/publications/health-matters-antimicrobial-resistance/health-matters-antimicrobial-resistance#contents [Accessed 08 10 2018].

Pullan, S. et al., 2007. Nitric Oxide in Chemostat-Cultured *Escherichia coli* Is Sensed by Fnr and Other Global Regulators: Unaltered Methionione Biosynthesis Indicates Lack of S Nitrosation. *Journal of Bacteriology,* 189(5), pp. 1845-55.

Puustinen, A. et al., 1991. Properties of the Two Terminal Oxidases of *Escherichia coli*. *Biochemistry,* pp. 3936-3942.

Rather, I., Kim, B., Bajpai, V. & al., e., 2017. Self-medication and antibiotic resistance: Crisis, current challenges, and prevention. *Saudi Journal of Biological Sciences,* 24(4), pp. 808-812.

Renggli, S., Keck, W., Jenal, U. & Ritz, D., 2013. Role of Autofluorescence in Flow Cytometric Analysis of *Escherichia coli* Treated with Bactericidal Antibiotics. *Journal of Bacteriology,* pp. 4067-4073.

Rogers, B., Sidjabat, H. & Paterson, D., 2011. *Escherichia coli* O25b-ST131: a pandemic, multiresistant, community-associated strain. *Journal of Antimicrobial Chemotherapy,* pp. 1-14.

Rolfe, M. et al., 2011. Transcript Profiling and Inference of *Escherichia coli* K-12 ArcA Activity across the Range of Physiologically Relevant Oxygen Concentrarions. *The Journal of Biological Chemistry,* pp. 10147-54.

Roszer, T., 2012. *The Biology of Subcellular Nitric Oxide.* Dordrecht: Springer Netherlands.

Safarian, S. et al., 2016. Structure of a bd oxidase indicates similar mechanisms for membrane-intergrated oxygen reductases. *Science,* 352(6285), pp. 583-586.

Schwarz, S., Kehrenberg, C., Doublet, B. & Cloeckaert, A., 2004. Molecular basis of bacterial resistance to chlormaphenicol and florfenicol. *FEMS Microbiology Reviews,* pp. 519-542.

Shephed, M., Sanguinetti, G., Cook, G. & Poole, R., 2010. Compensations for diminished terminal oxidase activity in *Escherchia coli*: cytochrome *bd*-II-mediated respiration and glutamate metabolism. *The journal of Biological Chemistry,* pp. 18464-72.

Shepherd, M. et al., 2016. The cytochrome *bd*-I respiratory oxidase augments survival of multidrug-resistant *Escherichia coli* during infection. *Scientific Reports,* 6(July), pp. 1-10.

Skold, O., 2000. Sulfonamide resistance: mechanisms and trends. *Drug Resistance Updates,* June, 3(3), pp. 155-160.

Sousa, P. et al., 2012. The aerobic respiratory chain of *Escherichia coli*: from genes to supercomplexes. *Microbiology,* Volume 158, pp. 2408-2418.

Speer, B., Shoemaker, N. & Salyers, A., 1992. Bacterial Resistance to Tetracycline: Mechanisms, Transfer, and Clinical Significance. *Clinical Microbiology Reviews,* pp. 387-399.

Spiro, S. & Guest, J., 1990. FNR and its role in oxygen-regulated gene expression in *Escherichia coli*. *FEMS Microbiology Reviews,* pp. 399-428.

Stevanin, T. et al., 2000. Flavohemoglobin Hmp Affords Inducible Protection for *Escherichia coli* Respiration, Catalyzed by Cytochromes *bo'* or *bd*, from Nitric Oxide. *The Journal of Biological Chemistry,* 275(46), pp. 35868-35875.

Sturr, M. G., Krulwich, T. A. & Hicks, D. B., 1996. Purification of a cytochrome *bd* terminal oxiase encoded by the *Escherichia coli app* locus from delta *cyo* delta *cyd* strain complemented by genes from *Bacillus firmus* OF4. *Journal of Bacteriology,* 178(6), pp. 1742-1749.

Sudhamsu, J. & Crane, B., 2009. Bacterial nitric oxide synthases: what are they good for?. *Trends in Microbiology,* May, 17(5), pp. 212-218.

Taber, H., Mueller, J., Miller, P. & Arrow, A., 1987. Bacterial Uptake of Aminoglycoside Antibiotics. *Microbial Reviews,* pp. 439-457.

Totsika, M. et al., 2011. Insights into a Multidrug Resistant *Escherichia coli* Pathogen of the Globally Disseminated ST131 Lineage: Genome Analysis and Virulence Mechanisms. *PLOS ONE,* p. e26578.

Tseng, C., Albrecht, J. & Gunsalus, R., 1996. Effect of microaerophillic cell growth conditions on expression of the aerobic (*cyoABCDE* and *cydAB*) and anaerobic (*narGHJI, frdABCD*, and *dmsABC*) respiratory pathway genes in *Escherichia coli*. *Journal of Bacteriology,* pp. 1094-8.

Unden, G. & Bongaerts, J., 1997. Alternative respiratory pathways of *Escherichia coli*: energetics and transcriptional regulation in response to electron acceptors. *Biochemicia et Biophysica Acta (BBA)- Bioenergetics,* pp. 217-234.

Van Acker, H. & Coenye, T., 2017. The Role of Reactive Oxygen Species in Antibiotic-Mediated Killing in Bacteria. *Trends in Microbiology.*

van den Berg, W., Hagen, W. & van Dongen, W., 2000. The hybrind-cluster protein ('prismane protein') from *Escherichia coli*. *European Journal of Biochemistry,* 267(3), pp. 666-676.

van Hengel, A. & Marin, L., 2019. Research, Innovation, and Policy: An Alliance Combating Antimicrobial Resistance. *Trends in Microbiology,* 27(4), pp. 287-289.

VanOrsdel, C. et al., 2013. The *Escherichia coli* CydX Protein is a Member of the CydAB Cytochrome *bd* Oxidase Complex and Is Required for Cytochrome *bd* Oxidase Activity. *Journal of Bacteriology,* pp. 3640-50.

Vine, C. & Cole, J., 2011. Unresolved sources, sinks, and pathways for the recovery of enteric bacteria from nitrosative stress. *FEMS Microbiology Letters,* 325(2), pp. 99-107.

Wang, H. & Gunsalus, R., 2000. The *nrfA* and *nirB* Nitrite Reductase Operons in *Escherichia coli* Are Expressed Differently in Response to Nitrate than to Nitrite. *Journal of Bacteriology,* Oct, 182(20), pp. 5813-5822.

Wang, J. et al., 2016. The roles of the hybrid cluster protein, Hcp and its reductase, Hcr, in high affinity nitric oxide reduction that protects anaerobic cultures of *Escherichia coli* against nitrosative stress. *Molecular Microbiology,* 100(5), pp. 877-892.

Wink, D., Hines, H., Cheng, R. & al, e., 2011. Nitric Oxide and redox mechanisms in the immune response. *Journal of Leukocyte Biology,* 89(6), pp. 873-891.

Wolfe, M., Heo, J., Garavelli, J. & Ludden, P., 2002. Hydroxylamine Reductase Activity of the Hybrid Cluster Protein from *Escherichia coli*. *Journal of Bacteriology,* 184(21), pp. 5898-902.

World Health Organization, 1999. *Containing Antimicrobail Resistance: Review of the Literature and Report of a WHO Workshop on the Development of a Global Strategy for the Containment of Antimicrobial Resistance,* Genneva: World Health Organization.

World Health Organization, 2014. *ANTIMICROBIAL RESISTANCE: Global Report on Surveillance,* s.l.: s.n.

Zhao, X. & Drlica, K., 2014. Reactive oxygen species and the bacterial repsonse to lethal stress. *Current Opinion in Microbiology,* pp. 1-6.

Appendix

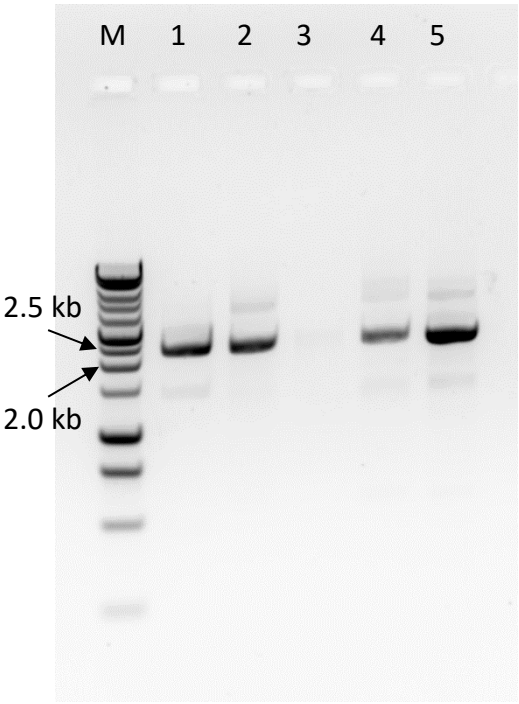

Figure A.1 Amplified Cm^R cassette from MS16. *5 µL of 4 colony PCR reactions (Lanes 1-4) aimed to amplify the Cm^R cassette present in place of the cydAB gene in MS16 were loaded onto a 1% agarose gel. Lane 5 contains the sequential elution of the 4 PCR reactions. The expected fragment length was 1995 bp.*

Figure A.2 Amplified Cm^R cassette from cyoA and appCB mutant strains. *5 µL of sequentially eluted Cm^R cassette from an appCB mutant, MS605, (Lane 1) and a cyoA mutant, MS506, (Lane 2) on 1% agarose gel. Expected length of the Cm^R cassette originating from MS605 is 2063 bp while expected the length of the Cm^R cassette from MS506 is 1950 bp*

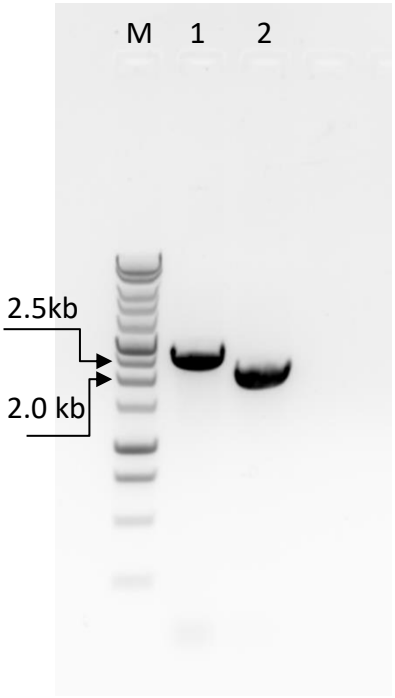

Figure A.3 Single mutant viability assay plates. *CFU/mL counts were conducted from colony counts. Three technical repeats from a biological repeat are displayed below from MS628 (bd-I only) in the presence (A) and absence (B) of GSNO; MS629 (bo') only in the presence (C) and absence (D) of GSNO; and MS630 (bd-II only) in the presence (E) and absence (F) of GSNO.*